ChemMedChem

Chemistry Europe
European Chemical Societies Publishing

Accepted Article

Title: 4,4,16-Trifluoropalmitate: design, synthesis, tritiation, radiofluorination and pre-clinical PET imaging studies on myocardial fatty acid oxidation

Authors: Matteo Zanda, Alessandro Colombano, Sergio Dall'Angelo, Lee Kingston, Gunnar Grönberg, Claudia Correia, Rossana Passannante, Zuriñe Baz, Miguel Angel Morcillo, Charles Elmore, and Jordi Llop

To be cited as: *ChemMedChem* 10.1002/cmdc.202000610

Link to VoR: https://doi.org/10.1002/cmdc.202000610

WILEY-VCH

4,4,16-Trifluoropalmitate: design, synthesis, tritiation, radiofluorination and pre-clinical PET imaging studies on myocardial fatty acid oxidation

Alessandro Colombano,[a] Sergio Dall'Angelo,[a] Lee Kingston,[b] Gunnar Grönberg,[c] Claudia Correia,[d] Rossana Passannante,[e] Zuriñe Baz,[e] Miguel Ángel Morcillo,[f] Charles S. Elmore,*[b] Jordi Llop,*[e],[g] Matteo Zanda*[a],[h],[§]

[a] Dr. Alessandro Colombano, Dr. Sergio Dall'Angelo, Prof. Dr. Matteo Zanda
Institute of Medical Sciences, University of Aberdeen, Aberdeen, Scotland, AB25 2ZD, UK
[b] Lee Kingston, Dr. Charles S. Elmore
Early Chemical Development, Pharmaceutical Science, R&D, AstraZeneca, 43183 Gothenburg (Sweden)
[c] Gunnar Grönberg
Medicinal Chemistry, Research and Early Development, Respiratory, Inflammation and Autoimmune, BioPharmaceuticals R&D, AstraZeneca, 43183 Gothenburg (Sweden)
[d] Dr. Claudia Correia
Bioscience Cardiovascular, Research and Early Development, Cardiovascular, Renal and Metabolism (CVRM), BioPharmaceuticals R&D, AstraZeneca, Gothenburg, Sweden
[e] Rossana Passannante, Zuriñe Baz, Dr. Jordi Llop
CIC biomaGUNE, Basque Research and Technology Alliance (BRTA), Paseo Miramon 182, 20014 San Sebastian (Spain)
[f] Dr. Miguel Ángel Morcillo
Biomedical Applications of Radioisotopes and Pharmacokinetics Unit, CIEMAT, 28040 Madrid (Spain)
[g] Dr. Jordi Llop
Centro de Investigación Biomédica en Red, Enfermedades Respiratorias – CIBERES, Av. Monforte de Lemos 3-5, 28029 Madrid (Spain)
[h] Prof. Dr. Matteo Zanda
C.N.R.-SCITEC, via Mancinelli 7, 20131 Milan (Italy)
[§] Prof. Dr. Matteo Zanda
Current address: Loughborough University, School of Science, Centre for Sensing and Imaging Science, Sir David Davies Building, Loughborough LE11 3TU, UK.
E-mail: m.zanda@lboro.ac.uk

Supporting information for this article is given via a link at the end of the document.

Abstract: Fatty acid oxidation (FAO) produces the majority of ATP used to sustain the cardiac contractile work, while glycolysis is a secondary source of ATP under normal physiological conditions. FAO impairment has been reported in the advanced stages of Heart Failure (HF) and is strongly linked to disease progression and severity. Thus, from a clinical perspective, FAO dysregulation provides prognostic value for HF progression, whose assessment could be used to improve patients' monitoring and therapy effectiveness. Positron emission tomography (PET) imaging represents a powerful tool for the assessment and quantification of metabolic pathways, *in vivo*. Several FAO PET tracers have been reported in the literature but none of them is in routine clinical use yet. Metabolically trapped tracers are particularly interesting, because they undergo FAO generating a radioactive metabolite, which is subsequently trapped in the mitochondria, thus providing a quantitative means of measuring FAO *in vivo*. Herein we describe the design, synthesis, tritium labelling and radiofluorination of 4,4,16-trifluoro-palmitate **1** as a novel potential metabolically trapped FAO tracer. Preliminary PET-CT studies on [^{18}F]**1** in rats showed rapid blood clearance, good metabolic stability – confirmed using [^{3}H]**1** in vitro – and resistance towards defluorination. However, cardiac uptake in rats was modest (0.24 ± 0.04% ID/g) and kinetic analysis showed reversible uptake, indicating that [^{18}F]**1** is not irreversibly trapped.

Introduction

Heart failure (HF) is a complex pathology that results from any structural or functional impairment of ventricular filling or ejection of blood[1]. During HF the cardiac pump function is unable to meet the body's needs and guarantee the optimal perfusion of tissues. It affects at least 26 million people worldwide[2] and depends on a variety of factors including aetiology, underlying coronary disease, and the presence of comorbidities such as obesity, hypertension and diabetes. There is no specific diagnostic test for HF and the diagnosis is based on a thorough clinical examination of the patient's clinical history and symptoms[3].

Adenosine triphosphate (ATP) is the main chemical fuel required for the contraction of the heart, which is strongly energy-demanding and continually requires ATP to sustain the contractile function. In the healthy heart, in normoxic conditions, almost 95% of ATP is produced through mitochondrial oxidative phosphorylation, with the remainder originating from glycolysis and the tricarboxylic acid (TCA) cycle[4]. The latter is fuelled by acetyl-CoA derived from glucose oxidation or from fatty acid β-oxidation (FAO), which accounts for at least 70% of the ATP production in the healthy adult heart. [5–7]

FAO is a highly regulated process that ultimately metabolises FAs in the mitochondrial matrix. Myocardial FAO can be influenced by many factors, such as the concentration of free FAs in plasma, hormonal status, oxygen availability and energy demand. The overall FAO rate depends on a multitude of processes, including FAs uptake into myocardium mediated by the FA transporter CD36, activation to corresponding thioesters by fatty acyl-CoA synthetase, incorporation in the intracardiac lipid pool by esterification, mitochondrial import by carnitine palmitoyltransferase I/II and carnitine acyltranslocase (CPT-I/CPT-II and CAT) and the four enzymes involved in the β-oxidation cycle[8]. CPT-I is a key enzyme involved in FAO and

CPT-I inhibitors, such as etomoxir or POCA (sodium 2-[5-(4-chlorophenyl)-pentyl]-oxirane-2-carboxylate), have been widely employed to reduce FAO rates in experimental studies.[9–12].
Analysis of data from HF patients proved to be challenging due to the diverse aetiology of the syndrome, concomitant comorbidities, numerous pharmacological therapies and clinical stage. Despite these difficulties, it is widely accepted that FAO decreases during HF progression and in late-stage HF[3,4,13–17], and one approach to investigate FAO non-invasively is by using positron emission tomography (PET). Contrary to other molecular imaging modalities, PET offers superb sensitivity and unlimited tissue penetration, and is fully quantitative and translational. Additionally, the administration of sub-pharmacological doses (sub-nanomolar range) of the contrast agent (radiotracer) suffices to acquire high quality images, thereby minimising the risk of toxic effects and avoiding interference with the physiological system under investigation[18–20].

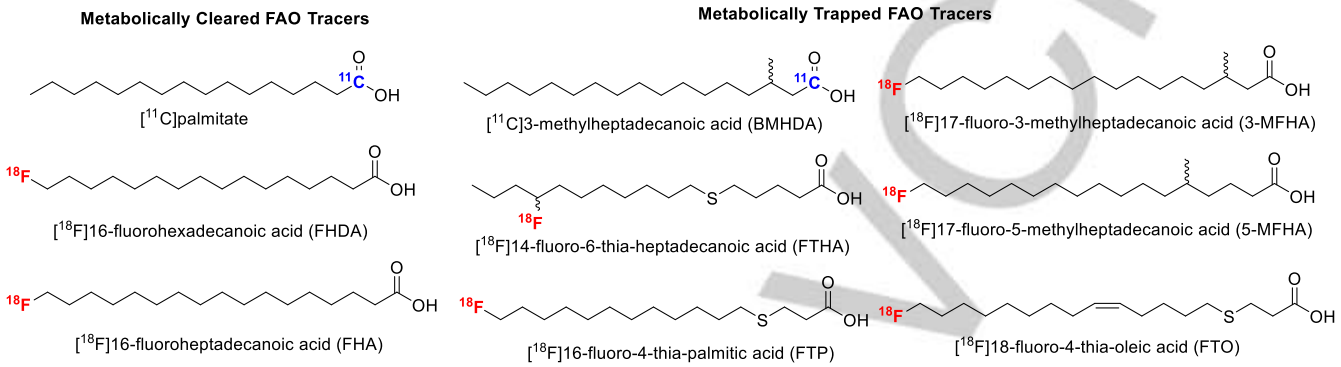

Figure 1. Examples of FAO tracers.

Myocardial FAO PET imaging has shown great potential in patients with ischemic heart disease, cardiomyopathies and heart failure[21,22], because it allows the assessment and quantification of regional tissue function *in vivo*, which usually precedes any anatomical changes during disease progression. [^{11}C]Palmitate (Fig. 1) has been extensively studied to monitor changes in metabolism in response to physiologic and pathologic conditions[23–27]. Complex mathematical modelling allows the estimation of tracer's uptake, oxidation and esterification[28]; however, quantitation in ischemic myocardium is not possible with this probe[29]. Long-chain FAs such as [^{18}F]FHDA and [^{18}F]FHA have also been developed, but the complex metabolic handling of these analogues, along with their *in vivo* defluorination, complicates the development of modelling strategies[30]. To simplify the myocardial kinetics, metabolically trapped probes have been developed. These compounds were designed so that they could be retained in the myocardium exclusively as metabolites formed due to β-oxidation, allowing for a close relationship between trapping rate and FAO rate. [^{11}C]BMHDA[31], [^{18}F]3-MFHA and [^{18}F]5-MFHA[32] are FA analogues with a methyl branch which have been designed to inhibit the β-oxidation cycle. However, these probes are poorly oxidised while being mainly incorporated into the intracardiac lipid pool, thus limiting their application as FAO tracers[22]. Fatty acids incorporating sulphur atoms have also been reported as metabolically trapped probes. [^{18}F]FTHA showed prolonged myocardial retention and FAO inhibition with a CPT-I inhibitor caused an 81% reduction in murine heart uptake, indicating specificity as FAO substrate[10]. However, this tracer has not been validated in the hypoxic myocardium, suggesting that FAO is not solely responsible for its accumulation[33]. [^{18}F]FTP showed specificity as β-oxidation substrate in normal and hypoxic perfused rat heart, despite suboptimal retention and high bone uptake, indicating extensive defluorination[34]. [^{18}F]FTO has been later reported with improved cardiac retention, even though the exact identity of the trapped metabolites is still unclear[9].
Additionally, compounds incorporating fluorine atoms or a cyclopropyl group have been reported in the literature[35,36], but their specificity for the FAO pathway still has to be clarified.
Herein we report the synthesis, tritium labelling, ^{18}F-labelling and preclinical evaluation of 4,4,16-trifluoro-palmitate (see Scheme 1), a novel FAO PET tracer candidate for cardiac imaging. The ^{18}F-labelled compound, **[^{18}F]1**, constitutes a fatty acid analogue with a [^{18}F]fluorine nuclide in ω-position and a geminal [^{19}F]difluoro group in position 4 of the hydrocarbon chain. These structural properties were carefully designed for the tracer to be taken up by the myocardium as a conventional fatty acid, e.g. as a FAO substrate. As shown in Fig. 2, the β-oxidation cycle was then expected to generate a reactive difluoroketone which would be trapped inside the mitochondria; hence, its accumulation would reflect the FAO rate. Difluoroketones can behave as transition state mimics and have been reported as enzymatic inhibitors, owing to the unique capability of binding in a substrate-like fashion in pockets on both sides of an enzyme's catalytic residues[37]. Additionally, the electrophilicity of the ketone carbonyl group is enhanced by the strong inductive effect of fluorine on the adjacent carbon atom[38], thus increasing the susceptibility to nucleophilic attack by mitochondrial enzymes and aminoacidic residues.

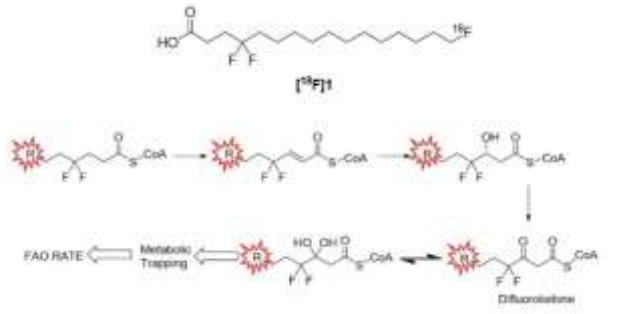

Figure 2. Working hypothesis of metabolic trapping of the PET tracer candidate [^{18}F]**1**. β-Oxidation metabolism was expected to generate a difluoroketone by sequential elimination, hydration and oxidation to difluoroketone of the parent compound.

Results and Discussion

CHEMISTRY

Synthesis of tritium labelling precursor 10 and non-radioactive tracer [^{19}F]1

Tritium labelling is an invaluable tool for performing preliminary in vitro studies on candidate PET tracers[39]. Since labelling with tritium can be readily performed by reduction of unsaturated hydrocarbons[40], we designed and synthesised compound **10** – which incorporates a double bond that can be tritiated by palladium-catalysed reduction with T_2 (Scheme 1) Additionally, the same synthetic route allowed us to prepare the non-radioactive version of the tracer [^{19}F]**1**, which was used as a reference for confirming the identity of the tracer [^{18}F]**1** by high performance liquid chromatography (HPLC). Several unsuccessful approaches to these compounds are described in the Supporting Information.

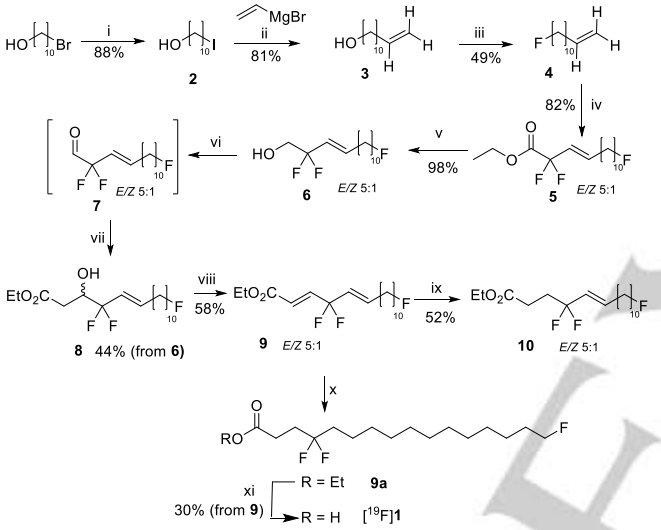

Scheme 1. Synthesis of compounds [^{19}F]**1** and **10**. Reagents and conditions: (i) NaI, acetone, reflux, 24 h; (ii) CuI, HMPA, $P(OEt)_3$, THF, -40 °C 1 h, 12 h rt; (iii) DAST, DCM, -30 °C 1 h, 12 h rt; (iv) $BrCF_2CO_2Et$, CuI, PMDETA, ACN, 100 °C, 12 h; (v) $NaBH_4$, EtOH, 2 h; (vi) oxalyl chloride, DMSO, TEA, DCM, -50 °C to rt, 1 h; (vii) $BrCH_2CO_2Et$, Zn, TMSCl, THF, reflux, 1 h; (viii) MsCl, TEA, DCM, 12 h, then DBU, 2 h; (ix) $[(C_6H_5)_3PCuH]_6$, toluene, 12 h; (x) H_2, Pd/C, MeOH, 12 h; (xi); LiOH, THF/H_2O 1:1; 12 h.

The preparation of the target compounds [^{19}F]**1** and **10** could be achieved via a multi-step process. First, commercially available 10-bromo-1-decanol was converted to the corresponding iodide **2** via a Finkelstein reaction following a published protocol[41]. Compound **2** was then treated with vinylmagnesium bromide to give **3,** which was deoxofluorinated with diethylaminosulfur trifluoride (DAST). The resulting terminal olefin **4** was submitted to difluoroalkylation with ethyl bromodifluoroacetate according to the methodology reported by Wang et al[42], yielding the key unsaturated ester **5** as 5:1 *E/Z* mixture of stereoisomers, as determined by NMR (see Experimental section). The intermediate aldehyde **7** was required as substrate for the subsequent Reformatsky reaction, but direct reduction of **5** to **7** with diisobutyl auminum hydride (DIBAL-H) was unsuccessful. However, this problem could be circumvented by full reduction to alcohol **6** with $NaBH_4$, followed by Swern oxidation to **7**. Reformatsky reaction with bromoacetate afforded the desired β-hydroxy ester **8**. Disappointingly, a variety of methods to directly deoxygenate **8** led to substrate decomposition, including Barton-McCombie deoxygenation with tributyltin hydride/ azobisisobutyronitrile (AIBN)[43], with triethylborane/diphenylsilane[44] or with indium chloride[45]. However, we observed that a stored batch of pure thiocarbonylimidazole xanthate derivative of **8**, synthesised for attempting a Barton-McCombie deoxygenation, spontaneously underwent elimination to the corresponding α,β-unsaturated derivative **9** upon storage at 10 °C. Thus, **8** was dehydrated by one-pot mesylation/elimination, affording the key intermediate **9**. Full hydrogenation of **9** followed by basic hydrolysis of the ethyl ester **9a** yielded the non-radioactive tracer [^{19}F]**1**, while its selective 1,4-conjugate reduction with the Stryker's reagent[46] afforded the tritium labelling precursor **10** as a 5:1 *E/Z* mixture of stereoisomers, as determined by NMR. Unexpectedly, hydrogenation of **9** using Pd/C in methanol afforded a mixture of desired compound **1** and 4,16-difluoropalmitate, which could be separated by supercritical fluid chromatography (SFC). It was later found that hydrogenation in THF completely suppressed the defluorination side-reaction.

Synthesis of fluorine labelling precursor 18

Fluorine-18 is commonly introduced in organic molecules by displacement of a good leaving group, such as a tosylate or a mesylate[47], by [^{18}F]fluoride. Thus, tosylate derivative **18** was identified as suitable fluorine labelling precursor, and successfully synthesised as shown in Scheme 2. Unsuccessful synthetic routes towards compound **18** are described in the Supporting Information.

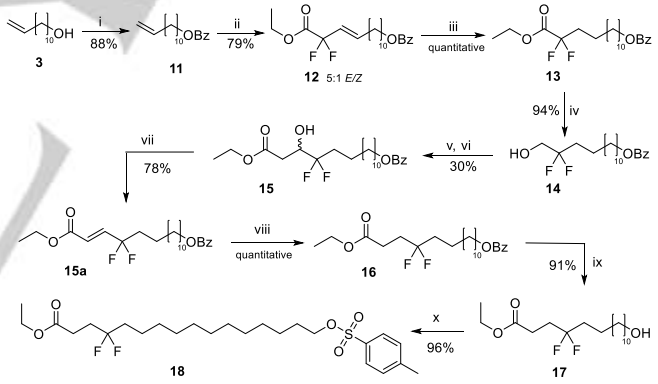

Scheme 2. Fluorine labelling precursor synthesis. Reagents and conditions: (i) BzCl, DMAP, pyridine, DCM, 1 h; (ii) $BrCF_2CO_2Et$, CuI, PMDETA, ACN, 100 °C, 12 h; (iii) H_2, Pd/C, THF, 12 h; (iv) $NaBH_4$, EtOH, 1 h; (v) oxalyl chloride, DMSO, TEA, DCM, -50 °C to rt, 1 h; (vi) $BrCH_2CO_2Et$, Zn, TMSCl, THF, reflux, 1 h; (vii) MsCl, TEA, DCM, 12 h, then DBU, 2 h; (viii) H_2, Pd/C, THF, 1 h; (ix) NaOEt, EtOH, 12 h; (x) TsCl, pyridine, DMAP, DCM, 12 h.

The unsaturated alcohol **3** was protected as benzoyl ester and successfully coupled with ethyl bromodifluoroacetate, affording ester **12** as a 5:1 mixture of *E/Z* stereoisomers. In analogy with the chemistry shown in Scheme 1, **12** was hydrogenated to **13**, which was reduced to **14** with $NaBH_4$ and used in a Reformatsky reaction with ethyl bromoacetate to afford **15**. The resulting secondary alcohol function was dehydroxylated in two steps to **16**, whose ω-hydroxy group was deprotected to give **17**. Finally, tosylation under standard conditions afforded the radiofluorination precursor **18**.

RADIOCHEMISTRY

Radiosynthesis of [^{3}H]1

A tritium labelled version of compound **1** was successfully prepared with the view of performing a preliminary *in vitro* evaluation of the tracer. With that aim, compound **10** was treated with tritium gas and 10% Pd/C as catalyst in THF (see **Fehler! Verweisquelle konnte nicht gefunden werden.**) to afford tritiated ethyl 4,4,16-palmitate, which was isolated by HPLC in 98.6% radiochemical purity. Subsequent basic hydrolysis of the ester function and HPLC purification afforded [^{3}H]**1** as a 36.7 MBq/mL solution in acetonitrile, with radiochemical purity higher than 99%.

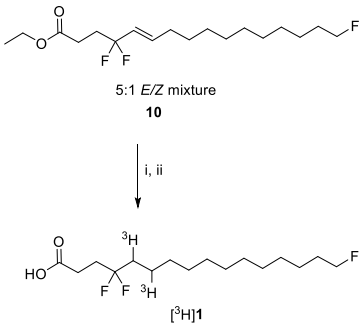

Scheme 3. Radiosynthesis of [^{3}H]**1**. Reagents and conditions: (i) $^3H_2$, 10% Pd/C, THF; (ii) LiOH, THF/H_2O.

The molar activity of [^{3}H]**1** was determined by NMR, according to the method of Schenk et al.[48], because its mass spectrum showed numerous isotopologues, suggesting that tritium incorporation had occurred in at least four positions of the molecule. This led to a mass spectrum which contained multiple overlapping isotopic patterns and any attempt to utilize this for determination of molar activity would have been accompanied by a large error[49]. The lack of a substantial UV chromophore negated the use of a standard mode of molar activity determination. Therefore, molar activity calculation by NMR using an internal standard seemed the best option and tritiated canagliflozin (1.3 Gbq/mmol molar activity, 91.7% radiochemical purity) was employed as internal standard. The method relied on the acquisition of ^{1}H and ^{3}H NMR spectra of a sample containing known amounts of [^{3}H]**1** and [^{3}H]canagliflozin; the molar activity was then calculated by comparison of ^{1}H and ^{3}H integrals of the two compounds.

A preliminary experiment was undertaken with the non-tritiated compounds dissolved in CD_3OD (Fig. 3). The resonances of two of the canagliflozin aromatic protons at 7.56 ppm and fluoromethylene doublets of triplets signal at 4.42 ppm of **1** were deemed to be ideal for the purpose because they are widely separated, well resolved and, importantly, not overlapping with the solvent signals. Moreover, the two canagliflozin thiophene ring tritium atoms (7.18 ppm, 6.77 ppm) are convenient for ^{3}H NMR comparison because they are well separated from the analyte aliphatic resonances (1.5 ppm).

Encouraged by these findings, carefully measured 100 MBq of standard and analyte were dissolved in deuterated methanol and ^{1}H/^{3}H NMR spectra were acquired (Fig. 4). Finally, integrals were compared as reported by Schenk et al.[48] and the calculated molar activity was found to be 2730 GBq/mmol. This result exceeded the maximum theoretical molar activity calculated for two tritium atoms (2131 GBq/mmol) and was consistent with multiple tritium incorporation, as inferred by MS analysis.

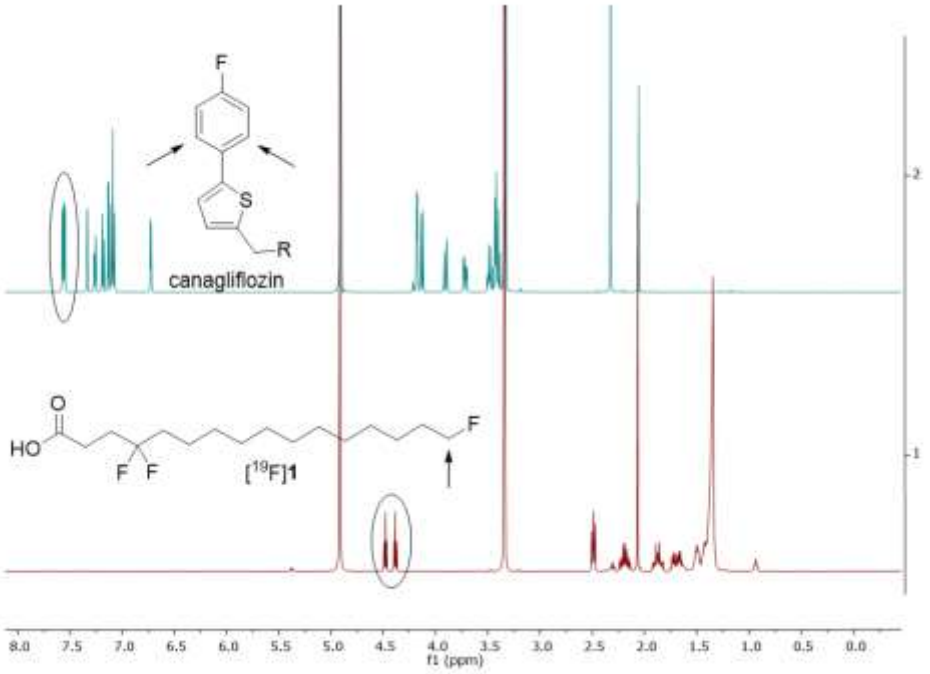

Figure 3. ^{1}H NMR spectra of **1** and canagliflozin in CD_3OD. Experiment 1 (bottom, red line) shows the fluoromethylene doublets of triplets signal of **1** (4.42 ppm). Experiment 2 (top, green line) shows two aromatic protons resonances of canagliflozin (7.56 ppm).

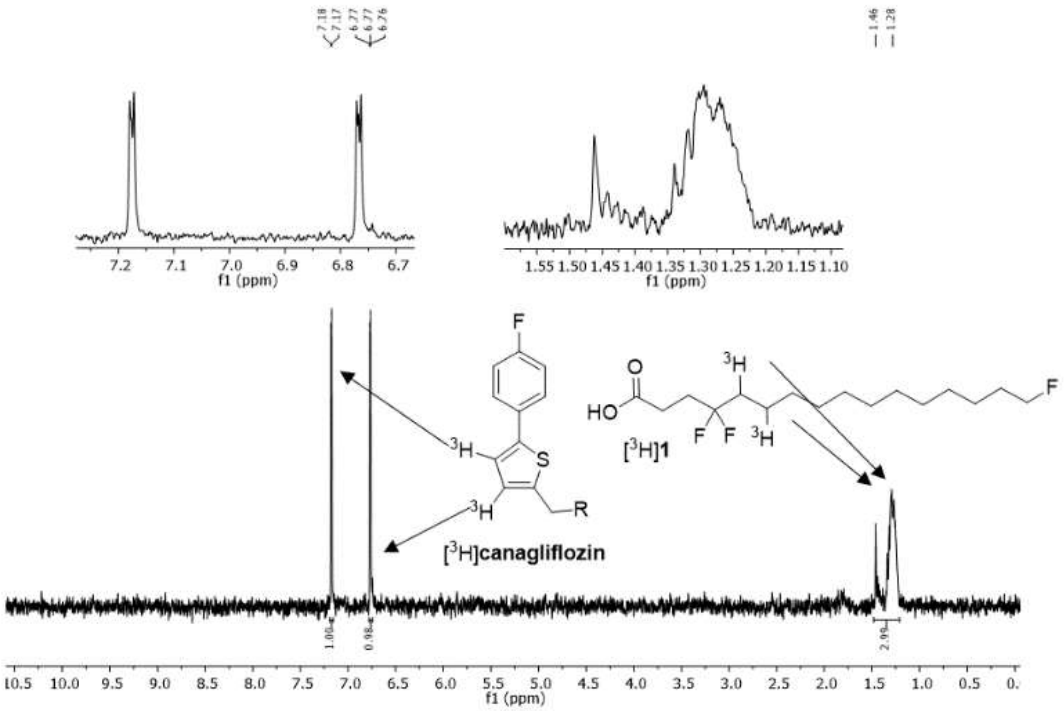

Figure 4. Proton decoupled ^{3}H NMR of [^{3}H]**1** and [^{3}H]Canagliflozin in CD_3OD. Aromatic signals for labelled canagliflozin are visible at 6.77 and 7.18 ppm. Aliphatic signals for [^{3}H]**1** are shown at 1.46 – 1.28 ppm.

In vitro metabolism

The tritium labelled compound was used to investigate hydroxylation metabolism, a minor metabolic pathway which has been described as being NADPH- dependent and catalyzed by the microsomal P450 enzyme family[50]. Experimentally, rat liver microsomes (ThermoFisher Scientific; 0.1mg of protein) were incubated with [^{3}H]**1** (0.36 MBq; 13 nmol) in the presence of NADPH as the cofactor, and the mixture was analyzed by radio-HPLC at 15, 30, 60, and 120 min. Initially, one major peak in the chromatogram was identified as [^{3}H]**1**, proving the radiochemical purity of the tracer. The appearance of a broad peak in the chromatogram with lower retention time at 15 min of incubation (Fig. 5.) confirmed the presence of metabolism. The percentage of the non-metabolized [^{3}H]**1** progressively decreased with incubation time, to reach values of ca. 25% at 2 hours of incubation (Fig. 5). The identity of the metabolites could not be confirmed. Cytochrome P450 enzymes are selective for C-H functionalization[51], hence the presence of free [^{18}F]fluoride due to fluorine-by-hydroxyl exchange can be excluded. Previous works reported in the literature have demonstrated that the presence of fluorine atoms in ω-position favour hydroxylation at the ω-3, ω-2 and ω-1 positions[52]. Hence, we hypothesize a major contribution of these hydroxylated metabolites.

Considering the values obtained at t=15 min of incubation, the initial metabolism rate was calculated to be 3.1 nmol/(mg min). It has been proven that the presence of fluorine atoms in ω-position stabilize the transition states of the hydroxylation reaction and therefore enhance reaction rates[51]. However, our values are in the range of those reported in the literature for lauric and oleic acid[50] under equivalent experimental conditions. Fitting of a mono-exponential curve to the experimental data showed the presence of a *plateau*, suggesting that a fraction of the fatty acid remains unchanged even at very long incubation times.

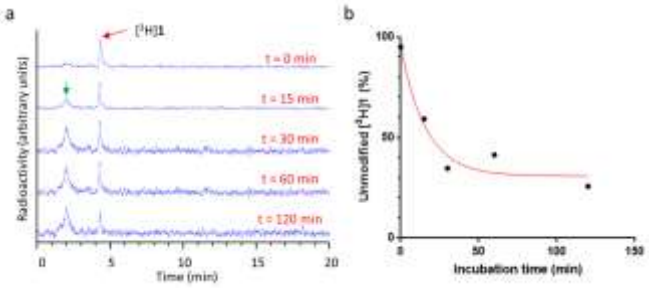

Figure 5. a) Chromatographic profiles obtained for [^{3}H]1 at different times after incubation with rat liver microsomes in the presence of NADPH. The peak corresponding to the metabolites is indicated with a green arrow; b) percentage of non-metabolised [^{3}H]1 as determined by integration of the area under the peaks in (a). In red, a mono-exponential equation fitted to the experimental data.

Radiosynthesis of [^{18}F]1

Further development of **1** into a tracer for *in vivo* PET imaging experiments required the incorporation of a positron emitter in ω-position. Hence, we next tackled the radiosynthesis of [^{18}F]**1**, which was achieved following a two-step process: [^{18}F]fluoride nucleophilic displacement of tosylate **18** first, followed by ethyl ester hydrolysis. Typical conditions reported in the literature for the preparation of other ^{18}F-labelled FAs involve heating the precursor and [^{18}F]fluoride in acetonitrile or THF solution, followed by additional heating in the presence of hydrochloric acid or potassium hydroxide to hydrolyse the protecting groups [9,34,35]. In our case, compound **18** was successfully radiolabelled using K_{222} as the phase transfer catalyst and acetonitrile as the solvent (Scheme 4). After ester hydrolysis with aqueous potassium hydroxide, purification by HPLC (Fig. S1b) and reformulation using solid phase extraction yielded the desired

tracer in 10-15% decay corrected radiochemical yield in an overall synthesis time of 70 min. Radiochemical purity was above 99%, as determined by radio-HPLC (Fig. S1a).

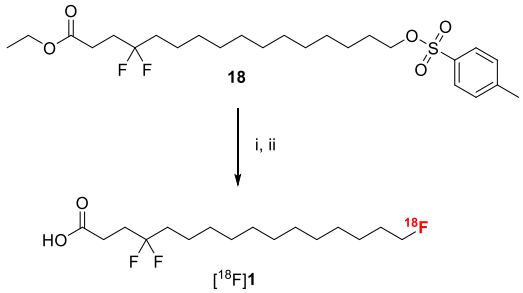

Scheme 4. Radiosynthesis of [^{18}F]**1**. Reagents and conditions: *(*i) [^{18}F]KF/K_{222}, ACN, 90 °C, 15 minutes; (ii) KOH, 90 °C, 5 minutes.

The radiotracer proved stable in physiological media, as determined by HPLC. Analysis at different times after incubation in the vehicle used for administration (1% bovine serum albumin –BSA– in physiological saline solution)[9,34] confirmed the presence of only one radioactive peak, corresponding to [^{18}F]**1**, up to six hours of incubation (Fig. S2).

IN VIVO STUDIES

Blood clearance and *in vivo* metabolism

New tracers require careful assessment of *in vivo* metabolism, as the formation of labelled metabolites complicates image interpretation and quantification[53]. Hence, we first explored blood clearance and tracer's metabolism *in vivo* using an in-house developed monitoring system (Fig. 6a) as previously described[54]. The system allows for the real-time determination of the concentration of radioactivity in arterial blood *via* extracorporeal circulation. Additionally, blood samples were withdrawn at preselected time points (5, 10, 15 and 30 minutes) for further processing.

Experimentally, 21 ± 2 MBq of [^{18}F]**1** solution in ethanol/1% BSA in physiologic saline solution (1:9, v:v) were injected into rats (n=2) through the femoral vein, concomitantly with the start of radioactivity measurements, which was prolonged over 30 minutes. Analysis of the withdrawn blood samples by HPLC showed excellent tracer metabolic stability *in vivo*, as no radioactive metabolites could be detected over the period studied (0-30 min; Fig. S3). Decay-corrected time activity curves (TACs) showed rapid clearance from the bloodstream at t<300 s (Fig. 6b). Interestingly, close-to-noise values were measured at t=450-900s, followed by an increase in radioactivity concentration at t>900 s which reached a maximum at t ~ 1300 s. This trend, which can be clearly visualised when the Y axis is represented in logarithmic scale (Fig. 6b), is consistent with the presence of enterohepatic circulation (see below for further discussion).

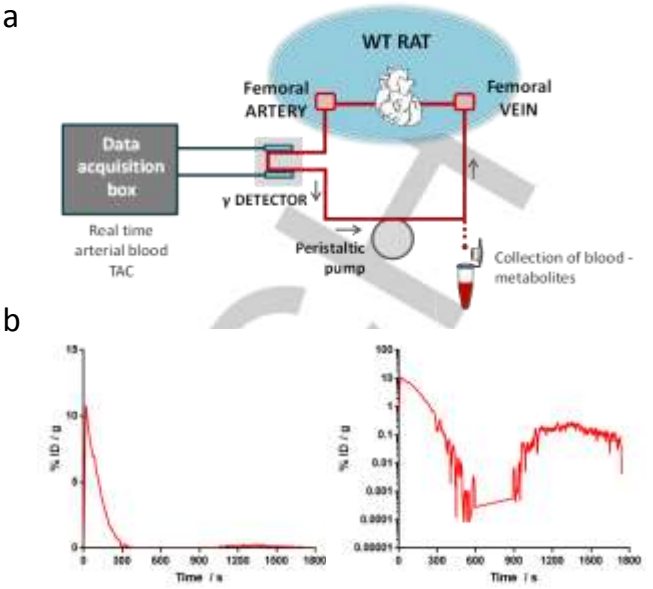

Figure 6. a) Schematic representation of the extracorporeal circulation system used for the determination of the arterial blood time-activity curve. Two catheters were inserted into the femoral artery and vein, respectively. The blood was pumped through a radioactive detector using a peristaltic pump. Blood samples were withdrawn at different time points to quantify the presence of metabolites; b) time-activity curves obtained after intravenous administration of [^{18}F]**1** in a healthy Sprague Dawley rat, expressed as a percentage of injected dose (%ID) per gram. Left: linear Y scale; right: logarithmic Y scale.

Imaging studies

To test whether [^{18}F]**1** would be subjected to oxidative metabolic trapping in the mitochondria *in vivo*, we decided to test whether etomoxir, a known CPT-I inhibitor, would cause any changes in the cardiac uptake of the tracer. We reasoned that if the tracer was a poor substrate for esterification and preferentially metabolized and retained in the mitochondria, a decreased retention of radioactivity upon pre-treatment with etomoxir would be observed.

With that aim, biodistribution and heart uptake of [^{18}F]**1** were investigated by PET imaging in healthy rats, which were pre-treated with etomoxir (n=5; "etomoxir" group) or the corresponding vehicle (n=5; "control" group) before tracer administration. Visual inspection of the images (Fig. 7a) showed the presence of the tracer in the blood pool at early time points after administration, and progressive accumulation of the radioactive signal in the liver (probably mediated by CD36, the physiological FA transporter) and in the gastrointestinal region, the latter more visible in the etomoxir pre-treated group. No accumulation of radioactivity was observed in bones, suggesting negligible *in vivo* defluorination, consistently with the excellent metabolic stability observed in metabolic *in vivo* studies.

In order to acquire quantitative data, representative volumes of interest (VOIs) were delineated in selected organs (liver, lungs, and kidneys; Fig. 7b). The image corresponding to the first frame (0-0.1 min) and averaged image of the last frames (8.4-60 min) enabled the delineation of VOIs in the caudal vena cava and the myocardium, respectively (Figure 7b). For all VOIs, the concentration of radioactivity as a function of time was determined (Fig. 7c). Consistently with the visual inspection of the images, a rapid accumulation of radioactivity was observed in the liver at early time points after administration, with a slightly higher concentration for the control group. TACs for the kidneys,

lungs and myocardium showed a high initial increase of radioactivity concentration (approx. 40 s after administration) followed by a fast clearance. Interestingly, a slight radioactivity increase was observed in these organs at late time points after tracer administration. However, this increase was more pronounced for control animals, and almost disappeared in the case of etomoxir-pre-treated animals. In line with results obtained by extracorporeal blood circulation, the image-derived blood TACs for control animals showed a fast peak at early time-points, a rapid clearance phase and finally a slight increase which was sustained over time (t > 10 min). The ratio between the average concentration of radioactivity in blood (C_b) in the time frames 2-5 min and 15-60 min ($Cp_{(2\text{-}5\ min)}/Cp_{(15\text{-}60\ min)}$) was 1.38 ± 0.11. This effect was not observed in etomoxir-treated animals, where ($Cp_{(2\text{-}5\ min)}/Cp_{(15\text{-}60\ min)}$) was 1.04 ± 0.08.

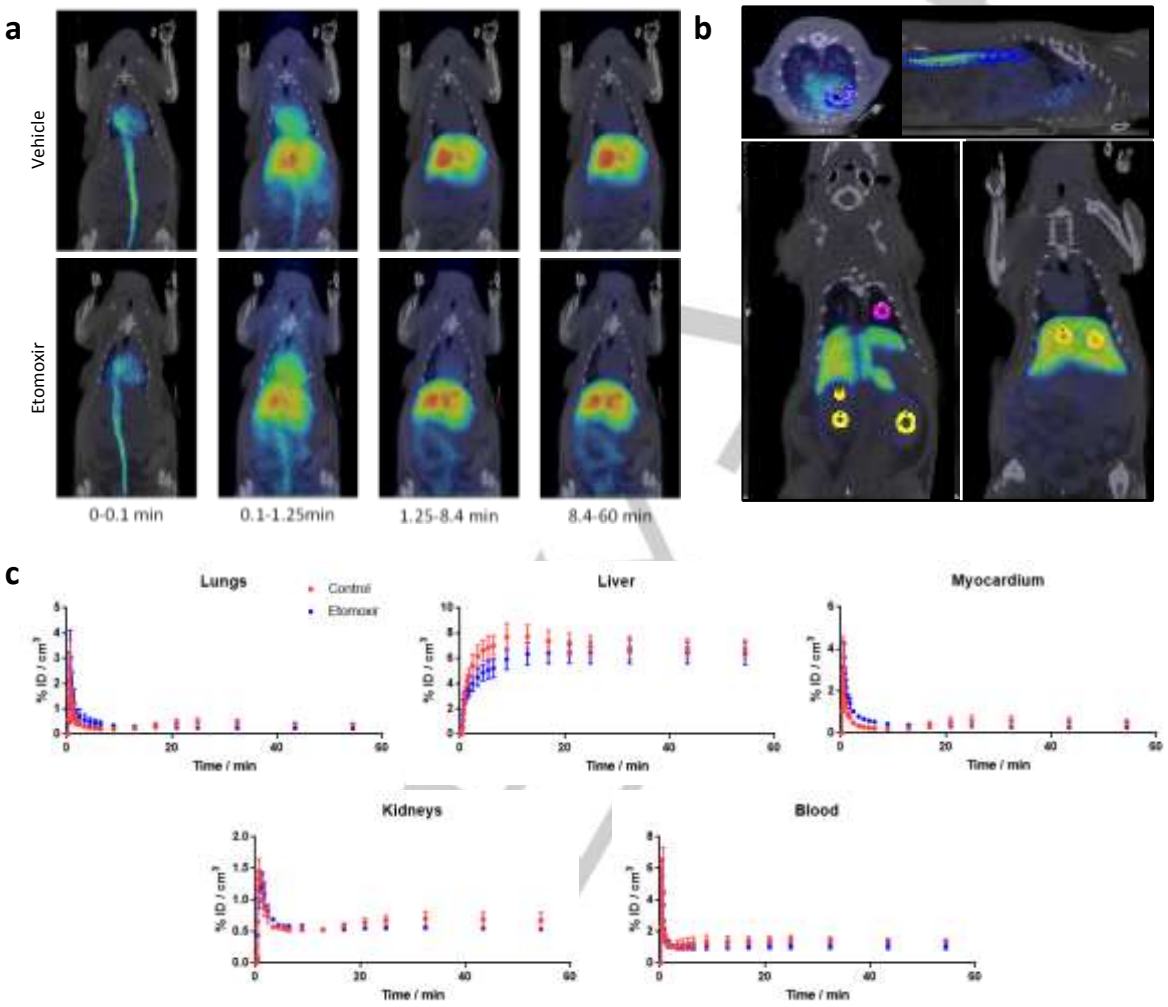

Figure 7. a) PET images (coronal projections) obtained at different time points after administration of compound [^{18}F]1 to rats pre-treated with vehicle (top) and etomoxir (bottom; dose = 40 mg/Kg). The images shown correspond to averaged frames in the indicated time-windows. PET images have been co-registered with representative CT slices for anatomical localization of the radioactive signal; b) representation of the volumes of interest (VOIs) drawn on the different organs to obtain dynamic time-activity curves; c) tracer time-activity curves in lungs, liver, blood, myocardium and kidneys, for animals pre-treated with vehicle (red; control group) and etomoxir (40 mg/Kg; blue; etomoxir group). Data are presented as mean ± standard deviation, n = 3 per experimental scenario.

The TAC profile observed in the blood from control animals and the accumulation of radioactivity in the liver observed at early time points, which suggest that the tracer is rapidly taken up by the hepatocytes, are compatible with *in vitro* metabolism results and the presence of enterohepatic circulation of [^{18}F]**1**. We hypothesize that after liver uptake, part of the tracer undergoes hydroxylation metabolism. Part of the intact tracer is secreted into the bile and released in the intestine, where the activity is reabsorbed into the systemic circulation. This process is probably assisted by hepatic conjugation/intestinal deconjugation[55]. The absence of metabolites in plasma up to t=30 min after administration suggests that the fraction of compound [^{18}F]**1** that undergoes enterohepatic circulation is not metabolised in the liver, or forms a conjugate in the liver which, after deconjugation in the gastro-intestinal region, results in the release of intact radiotracer into the systemic circulation. In animals pre-treated with etomoxir, enterohepatic circulation was not observed. The reasons behind this finding remain unclear and will be investigated in future works.

The rational design underlying the development of compound [^{18}F]**1** was to favour its metabolic trapping in the myocardium. Hence, TACs obtained in the myocardium were analysed using Patlak[56] graphical analysis (Fig. S4). However, the lack of a linear region suggested that the tracer is not irreversibly accumulated. Indeed, Logan analysis[57] of the cardiac TAC using the image-derived blood input function, showed profiles suggesting an equilibrium between the radioactivity in the heart and in the blood (Fig. 8). Average volume of distribution values

at equilibrium for control and etomoxir groups were 0.46 ± 0.11 and 0.39 ± 0.12, respectively. The difference between groups was not statistically significant (P = 0.505), suggesting that [^{18}F]**1** was not sensitive to FAO changes induced by etomoxir.

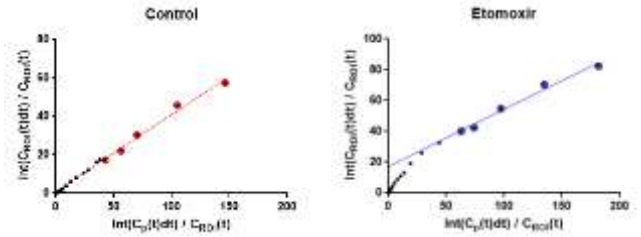

Figure 8. Representative Logan plots (myocardium) corresponding to the control group (left) and etomoxir group (right). In both cases, the plot was created using the image-derived blood input function. The points used for the linear regression are shown as coloured dots. T* = 20 minutes.

The similar cardiac accumulation observed between control and etomoxir group suggests that the tracer accumulation is not associated with β-oxidation processes. However, the reason behind the lack of differences between groups remains unresolved. This aspect could be clarified by e.g. analysis of radioactive metabolites in the heart at different time points, which may help to untangle the metabolic fate of the probe, or by inhibiting the different steps involved in the FAO process in order to gain mechanistic information about the *in vivo* behaviour of the new tracer.

Conclusion

In this study we have designed and developed a novel FAO PET tracer [^{18}F]**1**, for potential application in cardiac imaging. We successfully prepared the precursors for the isotope incorporation and radiolabelled the tracer with tritium and fluorine-18. [^{18}F]**1** showed highly desirable preliminary features such as straightforward radiosynthesis and smooth automated preparation which could be easily translated in routine radiochemistry facilities. Last, but not least, preliminary *in vivo* results indicated rapid uptake from the bloodstream and excellent *in vivo* metabolic stability. The preclinical results confirmed the fast radioactivity clearance from the bloodstream and the good metabolic stability.

Our working hypothesis was that [^{18}F]**1** would be metabolically trapped in the mitochondria, due to β-oxidation metabolism. However, the cardiac metabolism of FAs is a complex process, involving uptake and activation to corresponding fatty acyl-CoA, whose metabolic fate can be broadly distinguished between esterification to lipids or conversion to the corresponding carnitine derivatives by CPT-I for subsequent mitochondrial β-oxidation.

Unfortunately, kinetic analyses showed that the radiotracer uptake in the heart is subjected to dynamic equilibrium, rather than irreversible trapping. Moreover, the accumulation was not sensitive to CPT-I inhibition suggesting that its accumulation of [^{18}F]**1** was not associated with mitochondrial oxidative metabolism, which we hypothesised could be responsible for its metabolic trapping. Its retention in the heart may be due to other factors that would require further investigation.

Nevertheless, the introduction of fluorine atoms in fatty acids showed potential to provide metabolic stability. Thus, this strategy could be used for the development of the next generation FAO tracers or for the improvement of existing radiotracers.

Experimental Section

Chemistry

All reactions were carried out under nitrogen atmosphere and using dry solvents. Dry solvents were obtained from commercial sources and used without further purification. Reactions were monitored by thin-layer chromatography (TLC), unless otherwise noted. TLCs were performed on Merck silica gel glass plates (60 F254). Visualization was accomplished by UV light (254 nm) or staining with a ceric ammonium molybdate, KMnO4 and ninhydrin solution. Flash chromatography was performed using Silica gel (60 Å, particle size 40-63 μm) purchased from Merck. ^{1}H NMR and ^{13}C NMR spectra were recorded on a Bruker AVANCE III 400 NMR spectrometer and calibrated using residual non deuterated solvent as internal reference. ^{19}F NMR spectra were recorded on a Bruker AVANCE III 400 NMR spectrometer and were referenced to $CFCl_3$. ^{13}C NMR spectra were recorded with complete proton decoupling. Chemical shifts (δ) are reported in parts per million (ppm) and coupling constants (*J*) are given in Hertz (Hz). The following abbreviations are used for spin multiplicity: s = singlet, d = doublet, t = triplet, q = quartet, dd = doublet-doublet, dt = doublet-triplet, tt = triplet-triplet, m = multiplet, br = broad. When necessary, resonances were assigned using two-dimensional experiments (COSY and HSQC). Mass analyses were performed using Agilent 1200 HPLC system coupled to Agilent G6120 single quadrupole detector equipped with an electrospray ionization (ESI) source in direct infusion modality. ESI-MS spectra were recorded in positive mode, unless otherwise noted.

10-Iododecan-1-ol (2)

Compound synthesised according to the procedure reported by Karabiyikoglu et al.[41] Sodium iodide (19.5 g, 129 mmol, 3.5 eq) was added to a solution of 10-bromodecan-1-ol (7.4 mL, 37 mmol, 1 eq) in acetone (100 mL) and the mixture was refluxed for 24 hours. The reaction mixture was cooled to room temperature, diluted with water and extracted with EtOAc. The combined organic layers were washed with 1% $Na_2S_2O_3$ aq. solution, brine and dried over Na_2SO_4. Filtration and concentration under reduced pressure followed by flash chromatography (8:2 hexane/EtOAc) afforded the known alcohol (9.3 g, 88%) as white solid. Spectroscopic data were in agreement with literature values[41]. R_f 0.35 (8:2 hexane/EtOAc); ^{1}H NMR (400 MHz, CDCl3): δ = 3.64 (t, *J* = 6.8 Hz, 2H), 3.18 (t, *J* = 7.2 Hz, 2H), 1.81 (p, *J* = 7.2 Hz, 2H), 1.59-1.52 (m, 2H), 1.39-1.29 (m, 12H) (OH signal was not observed).

Dodec-11-en-1-ol (3)

Compound synthesised according to the procedure reported by Karabiyikoglu et al.[41] An oven-dried flask was charged with CuI (6.1 g, 32.0 mmol, 1 eq). THF (40 mL) was added and the suspension was cooled to -40 °C. A solution of vinylmagnesium bromide in THF (1M, 96.1 mL, 96.0 mmol, 3 eq) was added via cannula and the reaction was stirred for 15 minutes at -40 °C. Hexamethylphosphoramide (11.1 mL, 64.0 mmol, 2 eq), triethyl phosphite (11 mL, 64.0 mmol, 2 eq) and a solution of **2** (9.1 g, 32.0 mmol, 1 eq) in THF (50 mL) were then added sequentially dropwise via dropping funnel. The resulting mixture was stirred for 1 hour at -40 °C and allowed to warm to room temperature spontaneously overnight. The reaction was quenched with sat. aq. NH_4Cl solution (30 mL) and extracted with EtOAc. The organic layer was washed with brine and dried over Na_2SO_4. Filtration and concentration under reduced

pressure followed by flash chromatography (9:1 hexane/Et_2O) afforded the known colourless oil (4.60 g, 81%). Spectroscopic data were in agreement with literature values[41]. ^{1}H NMR (400 MHz, $CDCl_3$): δ = 5.81 (ddt, *J* = 17.0 Hz, 10.2, 6.8 Hz, 1H), 4.99 (ddt, *J* = 17.0, 2.2, 1.6 Hz, 1H), 4.92 (ddt, *J* = 10.2, 2.2, 1.2 Hz, 1H), 3.63 (t, *J* = 6.6 Hz, 2H), 2.06-2.00 (m, 2H), 1.60-1.53 (m, 2H), 1.41-1.28 (m, 14H) (OH signal was not observed).

12-Fluorododec-1-ene (4)

DAST (6.7 mL, 4.99 mmol, 2 eq) was added to a solution of **3** (4.6 g, 24.95 mmol, 1 eq) in DCM (50 mL) cooled to -30 °C. The reaction was stirred 1 hour at -30 °C and allowed to warm to room temperature overnight. The reaction was cooled to 0 °C, carefully quenched with sat. aq. $NaHCO_3$ solution (50 mL) and extracted with DCM. The organic layer was washed with brine, dried over Na_2SO_4 and concentrated under reduced pressure. Purification by flash chromatography (100% hexane to 8:2 hexane/EtOAc) afforded the title olefin (2.3 g, 49%) as a colourless oil. R_f 0.50 (100% hexane); ^{1}H NMR (400 MHz, $CDCl_3$): δ = 5.81 (ddt, *J* = 17.1 ,10.2, 6.7 Hz, 1H), 4.99 (ddt, J = 17.1, 2.1, 1.6 Hz, 1H), 4.92 (ddt, *J* = 10.2, 2.2, 1.2 Hz, 1H), 4.43 (dt, *J* = 47.5, 6.1 Hz, 2H), 2.10-1.98 (m, 2H), 1.77-1.59 (m, 2H), 1.47-1.20 (m, 14H); ^{13}C NMR (100 MHz, $CDCl_3$): δ = 139.4, 114.2, 84.3 (d, *J* = 163.0 Hz), 34.0, 30.6 (d, *J* = 19.2 Hz), 29.6 (3C), 29.4, 29.3, 29.1, 25.3 (d, *J* = 5.5 Hz); ^{19}F NMR (376 MHz, $CDCl_3$): δ -218.0 (tt, J = 47.5 Hz, 24.7 Hz, 1F).

Ethyl 2,2,14-trifluorotetradec-3-enoate (5)

Compound synthesised according to the methodology developed by Wang et al.[42] Acetonitrile (15 mL), CuI (144 mg, 0.755 mmol, 0.05 eq) and *N,N,N′,N″,N‴*-Pentamethyldiethylenetriamine (PMDETA) (4.7 mL, 22.7 mmol, 1.5 eq) were added into an oven-dried flask under nitrogen. The solution turned blue upon PMDETA addition. Ethyl bromodifluoroacetate (2.9 mL, 22.7 mmol, 1.5 eq) and a solution of **4** (2.82 g, 15.1 mmol, 1 eq) in acetonitrile (15 mL) were then added dropwise via dropping funnel and the mixture was heated at 100 °C for 12 hours. The reaction was filtered over celite washing with EtOAc and concentrated under reduced pressure. Purification by flash chromatography (95:5 hexane/EtOAc) afforded the title ester (3.81 g, 82%) as colourless oil as a 5:1 mixture of *E*/*Z* isomers. (*Z* isomer resonances are denoted by an asterisk). R_f 0.4 (95:5 hexane/EtOAc); ^{1}H NMR (400 MHz, $CDCl_3$): δ = 6.32 – 6.20 (m, 1H), 5.97 - 5.87* (m, 0.2H), 5.75 – 5.63 (m, 1H), 5.62 – 5.54* (m, 0.2H), 4.42 (dt, *J* = 47.4 Hz, 6.2 Hz, 2.4H), 4.31 (q, *J* = 7.1 Hz, 2.4H), 2.34 – 2.24* (m, 0.4H), 2.21 – 2.10 (m, 2.2H), 1.79 – 1.62 (m, 2.4H), 1.49 – 1.25 (m, 20.4H); ^{13}C NMR (100 MHz, $CDCl_3$): δ 164.3 (t, *J* = 34.9 Hz), 142.5* (t, *J* = 7.1 Hz), 140.1 (t, *J* = 8.8), 121.1 (t, *J* = 24.8 Hz), 121.0* (t, *J* = 26.2 Hz), 112.5 (t, *J* = 246.0 Hz), 84.2 (d, *J* = 163.0 Hz), 63.0, 32.0, 30.5 (d, *J* = 19.3 Hz), 29.6, 29.5, 29.5*, 29.4, 29.3, 29.2* (2C), 29.1, 28.5*, 28.2, 25.2 (d, *J* = 5.5 Hz), 14.1; ^{19}F NMR (376 MHz, $CDCl_3$): δ = -98.8* (m, 0.4F), -102.9 (m, 2F), -218.0 (m, 1.2F); MS (ESI, *m/z*): calcd. for $C_{16}H_{27}F_3O_2Na$ $[M+Na]^+$: 331.19, found 330.9.

2,2,14-Trifluorotetradec-3-en-1-ol (6)

$NaBH_4$ (690 mg, 18.1 mmol, 1.5 eq) was added portion wise to a solution of **5** (3.72 g, 12.0 mmol, 1 eq) in ethanol (40 mL) cooled to 0 °C and the reaction was stirred at room temperature. After 2 hours the reaction was cooled to 0 °C and quenched with sat. aq. NH_4Cl solution. The mixture was extracted with EtOAc and the combined organic layers were washed with brine, dried over Na_2SO_4 and concentrated under reduced pressure. Purification by flash chromatography (8:2 hexane/EtoAc) afforded the title compound (3.1 g, 98%) as colourless oil as a 5:1 mixture of *E*/*Z* isomers. (*Z* isomer resonances are denoted by an asterisk). R_f 0.35 (8:2 hexane/EtOAc); ^{1}H NMR (400 MHz, $CDCl_3$): δ = 6.23-6.11 (m, 1H), 5.90-5.80* (m, 0.2H), 5.65-5.52 (m, 1H), 5.51-5.42* (m, 0.2H), 4.43 (dt, *J* = 47.4 Hz, 6.2 Hz, 2.4H), 3.83-3.70 (m, 2.4H), 2.31-2.20* (m, 0.4H), 2.18-2.07 (m, 2H), 2.04-1.92 (m, 1.2H), 1.76-1.60 (m, 2.4H), 1.50-1.21 (m, 17.2H); ^{13}C NMR (100 MHz, $CDCl_3$): δ 140.9* (t, *J* = 5.6 Hz), 138.6 (t, *J* = 9.5 Hz), 122.2 (t, *J* = 25.4 Hz), 121.7* (t, *J* = 25.4 Hz), 120.4* (t, *J* = 239.4 Hz), 119.5 (t, *J* = 237.8 Hz), 84.3 (d, *J* = 162.9 Hz), 65.2 (t, *J* = 32.5 Hz), 32.1, 30.5 (d, *J* = 19.1 Hz), 29.6, 29.5, 29.4, 29.3, 29.2, 28.5, 25.1 (d, *J* = 5.5 Hz); ^{19}F NMR (376 MHz, $CDCl_3$): δ -102.2* (m, 0.4F), -105.9 (m, 2F), -218.0 (m, 1.2F); MS (ESI, *m/z*): calcd. for $C_{14}H_{25}F_3ONa$ $[M+Na]^+$: 289.19, found 289.1

Ethyl 4,4,16-trifluoro-3-hydroxy-hexadec-5-enoate (8)

Compound synthesised according to a modified reported procedure.[58,59] A solution of oxalyl chloride (1.0 mL, 11.49 mmol, 3 eq) in DCM (8 mL) was cooled to -50 °C and DMSO (1.6 mL, 22.9 mmol, 6 eq) was carefully added dropwise. The solution was vigorously stirred for 2 minutes at -50 °C and then warmed to -30 °C. A solution of **6** (1.02 g, 3.83 mmol, 1 eq) in DCM (10 mL) was then added dropwise via dropping funnel over 10 minutes. The resulting mixture was stirred for additional 30 minutes at -30 °C, then TEA (6.4 mL, 45.96 mmol, 12 eq) was added dropwise via dropping funnel over 10 minutes. The reaction mixture was then stirred for additional 30 minutes at -30 °C and allowed to warm to room temperature in one hour via removal of the external cooling bath. The reaction was quenched with sat. aq. NH_4Cl solution, diluted with water and extracted with DCM. The combined organic layers were washed with sat. aq. $NaHCO_3$ solution, water, brine, dried over Na_2SO_4 and concentrated under reduced pressure to give the crude aldehyde as a yellow oil. The crude product **7** was used without further purification. Zinc dust (0.62 g, 9.55 mmol, 2.5 eq) was suspended in THF (12.5 mL) and the suspension stirred for 5 minutes. TMSCl (180 µL, 1.43 mmol, 0.375 eq) was then added and the resulting mixture stirred for 15 minutes. The reaction was gently heated with a heat gun for 1 minutes under nitrogen flow and allowed to cool back to room temperature (three times). A solution of the freshly prepared aldehyde **7** (1.01 g, 3.82 mmol, 1 eq) in THF (10 mL) and ethyl bromoacetate (640 µL, 5.73 mmol, 1.5 eq) were consecutively added dropwise and the resulting suspension was refluxed for 1.5 hours. The reaction was quenched with sat. aq. NH_4Cl solution, filtered over celite and extracted with Et_2O. The combined organic layers were washed with water, brine, dried over Na_2SO_4 and concentrated under reduced pressure. Purification by flash chromatography (85:15 hexane/EtOAc) afforded the title β-hydroxy-ester (590 mg, 44% over two steps) as a yellow oil as a 5:1 mixture of *E*/*Z* isomers. (*Z* isomer resonances are denoted by an asterisk). R_f = 0.5 [8:2 Hexane/EtOAc]; ^{1}H NMR (400 MHz, $CDCl_3$): δ = 6.25-6.10 (m, 1H), 5.93-5.82* (m, 0.2H), 5.71-5.55 (m, 1H), 5.55-5.43* (m, 0.2H), 4.42 (dt, *J* = 47.4 Hz, 6.2 Hz, 2.4H), 4.31-4.13 (m, 3.6H), 3.20-3.06 (m, 1.2H), 2.72-2.48 (m, 2.4H), 2.33-2.21* (m, 0.4H), 2.19-2.06 (m, 2H), 1.78-1.57 (m, 2.4H), 1.50-1.22 (m, 20.4H); ^{13}C NMR (100 MHz, $CDCl_3$): δ 171.7, 140.9* (t, *J* = 5.5 Hz), 138.5 (t, *J* = 8.8 Hz), 121.3 (t, *J* = 24.6 Hz), 120.7* (t, *J* = 24.7 Hz), 120.5* (dd, *J* = 243.9 Hz, 241.7 Hz), 119.5 (dd, *J* = 241.9 Hz, 240.5 Hz), 84.2 (d, *J* = 163.0 Hz), 70.4 (dd, *J* = 31.8 Hz, 30.8 Hz), 62.1, 35.2 (t, *J* = 2.2 Hz), 34.9* (t, *J* = 2.8 Hz), 32.0, 30.4 (d, *J* = 19.1 Hz), 29.4 (2C), 29.3, 29.2, 29.1, 28.3, 25.1 (d, *J* = 5.5 Hz), 14.2; ^{19}F NMR (376 MHz, $CDCl_3$): δ -101.3 – -102.2* (m, 0.2F), -105.0 – -105.8 (m, 1F), -106.3 – -107.1* (m, 0.2F), -110.6 – -111.4 (m, 1F), -217.9 (m, 1.2F); MS (ESI, *m/z*): calcd. for $C_{18}H_{31}F_3O_3Na$ $[M+Na]^+$: 375.22, found 375.2; calcd. for $C_{18}H_{31}F_2O_3$ $[M-F]^+$: 333.22, found 333.2.

Ethyl 4,4,16-trifluorohexadeca-2,5-dienoate (9)

TEA (540 µL, 3.88 mmol, 2.5 eq) and MsCl (180 µL, 2.33 mmol, 1.5 eq) were added dropwise to a solution of **8** (546 mg, 1.55 mmol, 1 eq) in DCM (5 mL) cooled to 0 °C. The reaction was stirred for 12 hours at room temperature. The mixture was then cooled to 0 °C, DBU (460 µL, 3.1 mmol, 2 eq) was added dropwise and the mixture was stirred for 2 additional hours at room temperature. The reaction was quenched with sat. aq. $NaHCO_3$ solution and extracted with DCM. The organic layer was washed with sat. aq. $NaHCO_3$ solution and brine, dried over Na_2SO_4 and concentrated under reduced pressure. Purification by flash chromatography (98:2 hexane/EtOAc) afforded the title α,β-unsaturated

ester (300 mg, 58%) as a colourless oil as 5:1 mixture of *E*/*Z* isomers. (*Z* isomer resonances are denoted by an asterisk). R_f 0.4 (95:5 hexane/EtOAc); ^{1}H NMR (400 MHz, $CDCl_3$): δ = 6.85 (dt, *J* = 15.8 Hz, 10.3 Hz, 1.2H), 6.27 (dt, *J* = 15.8 Hz, 2.2 Hz, 1.2H), 6.18-6.07 (m, 1H), 5.90-5.80* (m, 0.2H), 5.70-5.46 (m, 1.2H), 4.45 (dt, *J* = 47.4 Hz, 6.2 Hz, 2.4H), 4.26 (q, *J* = 7.2 Hz, 2.4H), 2.26-2.17* (m, 0.4H), 2.17-2.07 (m, 2H), 1.78-1.61 (m, 2.4H), 1.48-1.23 (m, 20.4H); ^{13}C NMR (100 MHz, $CDCl_3$): δ 165.3, 140.4* (t, *J* = 7.2 Hz), 139.6* (t, *J* = 30.4 Hz), 139.5 (t, *J* = 30.0 Hz), 138.5 (t, *J* = 8.8 Hz), 124.9 (t, *J* =7.9 Hz), 124.4* (t, *J* = 8.2 Hz), 123.7 (t, *J* = 27.9 Hz), 123.0* (t, *J* = 28.6 Hz), 117.4 (t, *J* = 234.0 Hz), 84.2 (d, *J* = 163.0 Hz), 61.2, 32.0, 30.6 (d, *J* = 5.4 Hz), 29.6, 29.5, 29.4, 29.3, 29.2, 28.4, 25.2 (d, *J* = 5.4 Hz), 14.2; ^{19}F NMR (376 MHz, $CDCl_3$): δ -90.11 — -90.23* (m, 0.4F), -94.07 — -94.23 (m, 2F), -218.02 (m, 1.2F); MS (ESI, *m/z*): calcd. for $C_{18}H_{29}F_3O_2Na$ $[M+Na]^+$: 357.21, found 357.1; calcd. for $C_{18}H_{30}F_3O_2$ $[M+H]^+$: 335.21, found 335.2

Ethyl 4,4,16-trifluorohexadecanoate (9a)

10% Pd/C (10 mg) was added to a degassed solution of **9** (83 mg, 0.25 mmol) in methanol (1 mL); the round-bottom flask was purged with hydrogen and stirred overnight at room temperature. The reaction mixture was filtered over celite, concentrated under reduced and purified by flash chromatography (95:5 hexane/ EtOAc). The crude ester was used in the next step without further purification. An analytical sample was purified by preparative SFC using a Chiralpak IG column (250 x 20 mm, 5 µm); mobile phase consisted of 10% MeOH\Formate 20 mM in CO_2, 120 bar with an isocratic gradient and a flow of 70 mL\min. R_f 0.29 (95:5 hexane/EtOAc); ^{1}H NMR (500 MHz, $CDCl_3$): δ 4.46 (dt, *J* = 47.4, 6.2 Hz, 2H), 4.17 (q, *J* = 7.1 Hz, 2H), 2.54 (t, *J* = 2.4 Hz, 2H), 2.27 – 2.09 (m, 2H), 1.91 – 1.78 (m, 2H), 1.77 – 1.65 (m 2H), 1.53 – 1.45 (m, 2H), 1.45 – 1.18 (m, 19H); ^{13}C NMR (126 MHz, CDCl3) δ 172.6, 124.4 (t, *J* = 240.8 Hz), 84.3 (d, *J* = 163.9 Hz), 60.7, 36.7 (t, *J* = 25.0 Hz), 31.6 (t, *J* = 25.9 Hz), 30.4 (d, *J* = 19.4 Hz), 29.6, 29.5, 29.4 (2C), 29.3, 29.3, 27.3 (t, *J* = 4.7 Hz), 25.2 (d, *J* = 5.6 Hz), 22.3 (d, *J* = 4.5 Hz), 14.2; ^{19}F NMR (471 MHz, $CDCl_3$) δ -99.8 (p, *J* = 16.8 Hz, 2F), -218.0 (tt, *J* = 47.4, 24.9 Hz, 1F); MS (ESI, *m/z*): calcd. for $C_{18}H_{33}F_2O_2$ $[M-F]^+$: 319.24, found 319.3.

Ethyl 4,4,16-trifluorohexadec-5-enoate (10)

To a solution of (triphenylphosphine)copper hydride hexamer (Stryker's reagent) (440 mg, 22.5 mmol, 0.3 eq) in toluene (5 mL) cooled to 0 °C was added a solution of **9** (250 mg, 74.9 mmol, 1 eq) in toluene (1 mL) dropwise. The red suspension was stirred for 12 hours at room temperature. After 12 hours further 0.3 equivalents of Stryker's reagent were added and the suspension was stirred for additional 3 hours. The reaction was quenched by stirring at open air for 1 hour and subsequently filtered over celite. Purification by flash chromatography (95:5 hexane/ Et_2O) afforded the title compound (130 mg, 52%) as a colourless oil as 5:1 mixture of *E*/*Z* isomers. (*Z* isomer resonances are denoted by an asterisk). R_f 0.2 (95:5 hexane/Et_2O); ^{1}H NMR (400 MHz, $CDCl_3$): δ 6.13-6.00 (m, 1H), 5.78-5.68* (m, 0.2H), 5.59-5.35 (m, 1.2H), 4.45 (dt, *J* = 47.4 Hz, 6.2 Hz, 2.4H), 4.14 (q, *J* = 1.8 Hz, 2.4H), 2.54-2.42 (m, 2.4H), 2.34-2.16 (m, 2.8H), 2.13-2.03 (m, 2H), 1.76-1.57 (m, 2.4H), 1.44-1.20 (m, 20.4H); ^{13}C NMR (100 MHz, $CDCl_3$): δ 172.5, 139.1* (t, *J* = 6.2 Hz), 136.8 (t, *J* = 9.2 Hz), 124.6 (t, *J* = 26.2 Hz), 124.1* (t, *J* = 26.5 Hz), 121.9* (t, *J* = 238.2 Hz), 120.9 (t, *J* = 236.4 Hz), 84.4 (d, *J* = 163.0 Hz), 60.8, 33.8* (t, *J* = 27.5 Hz), 32.8 (t, *J* = 27.6 Hz), 31.9, 30.5 (d, *J* = 19.2 Hz), 29.6, 29.5 (2C), 29.4 ,29.2, 28.6, 28.4*, 27.8 (t, *J* = 4.3 Hz), 27.6* (t, *J* = 4.0 Hz), 25.3 (d, *J* = 5.4 Hz), 14.2; ^{19}F NMR (376 MHz, $CDCl_3$): δ -92.31 — -92.5* (m, 0.4F), -96.06 — -94.30 (m, 2F), -218.02 (m, 1.2F); MS (ESI, *m/z*): calcd. for $C_{18}H_{31}F_3O_2Na$ $[M+Na]^+$: 359.23, found 359.2; calcd. for $C_{18}H_{31}F_2O_2$ $[M-F]^+$: 317.23, found 317.2.

4,4,16-Trifluorohexadecanoic acid (1)

To a solution of crude **9a** (50 mg, 0.14 mmol, 1 eq) in THF\water 1:1 (1 mL) was added lithium hydroxide (5 mg, 0.22 mmol, 1.5 eq) and the suspension was stirred overnight at room temperature. The mixture was acidified with HCl 1 N aqueous solution to pH 2 and extracted with EtOAc; the organic layer was dried over Na_2SO_4 and concentrated under reduced pressure. The crude acid was purified by preparative SFC using a Chiralpak IG column (250 x 20 mm, 5 µm); mobile phase consisted of 10% MeOH\Formate 20 mM in CO_2, 120 bar with an isocratic gradient and a flow of 70 mL\min. The title compound (14 mg, 30%) was isolated as a white solid. R_f 0.2 (6:4 hexane/EtOAc); ^{1}H NMR (500 MHz, $CDCl_3$) δ 4.46 (dt, *J* = 47.4, 6.2 Hz, 2H), 2.59 – 2.64 (m, 2H), 2.20 (tt, *J* = 16.6 Hz, 7.8 Hz, 2H), 1.79 – 1.93 (m, 2H), 1.63 – 1.77 (m, 2H), 1.45 – 1.53 (m, 2H), 1.38 – 1.44 (m, 2H), 1.25 – 1.37 (m, 14H); ^{13}C NMR (126 MHz, CDCl3) δ 178.2, 124.2 (t, *J* = 240.8 Hz), 84.3 (d, *J* = 163.8 Hz), 36.7 (t, *J* = 24.9 Hz), 31.3 (t, J = 25.9 Hz), 30.4 (d, *J* = 19.3 Hz), 29.5 (2C), 29.4 (2C), 29.3, 29.2, 27.0, 25.1 (d, *J* = 5.5 Hz), 22.3 (t, *J* = 4.5 Hz); ^{19}F NMR (471 MHz, $CDCl_3$) δ -100.0 (p, *J* = 16.7 Hz, 2F), -218.2 – -217.8 (tt, *J* = 47.4, 24.9 Hz, 1F); MS (ESI, *m/z*): calcd. for $C_{16}H_{28}F_3O_2$ $[M-H]^-$: 309.21, found 309.3.

Dodec-11-enyl benzoate (11)

To a solution of **3** (51 mg, 0.28 mmol, 1 eq) and DMAP (3.4 mg, 0.028 mmol, 0.1 eq) in DCM (0.5 mL) were added pyridine (45 µL, 0.55 mmol, 2 eq) and benzoyl chloride (48 µL, 0.42 mmol, 1.5 eq) at 0 °C dropwise; the reaction was stirred at room temperature. After one hour the reaction was quenched with sat. acq. $NaHCO_3$ solution and the mixture was extracted with EtOAc; the organic layer was washed with sat. aq. $NaHCO_3$ solution and brine, dried over Na_2SO_4 and concentrated under reduced pressure. Purification by flash chromatography (98:2 hexane/EtOAc) afforded the protected alcohol (80 mg, 88%) as colourless oil. R_f 0.35 (98:2 hexane/EtOAc); ^{1}H NMR (400 MHz, $CDCl_3$): δ = 8.10-8.00 (m, 2H), 7.58 - 7.50 (m, 1H), 7.47-7.39 (m, 2H), 5.81 (ddt, *J* = 6.6 Hz, 10.3 Hz, 17.0 Hz, 1H), 4.99 (ddt, *J* = 17.1, 2.1, 1.6 Hz, 1H), 4.93 (ddt, *J* = 10.2, 2.2, 1.2 Hz, 1H), 4.31(t, *J* = 6.7 Hz, 2H), 2.09-1.98 (m, 2H), 1.77 (p, J = 6.8 Hz, 2H), 1.5-1.22 (m, 14H); ^{13}C NMR (100 MHz, $CDCl_3$): δ = 168.8, 139.3, 132.9, 130.7, 129.7, 128.4, 114.2, 65.2, 33.9, 29.6 (3C), 29.4, 29.2, 29.0, 28.8, 26.2; MS (ESI, *m/z*): calcd. for $C_{19}H_{28}O_2Na$ $[M+Na]^+$: 311.21, found 311.2.

[14-Ethoxy-13,13-difluoro-14-oxo-tetradec-11-enyl] benzoate (12)

Compound synthesised according to the methodology developed by Wang et al.[42] Acetonitrile (33 mL), CuI (126 mg, 0.66 mmol, 0.05 eq) and PMDETA (4.1 mL, 19.8 mmol, 1.5 eq) were added into an oven-dried flask under nitrogen. The solution turned blue upon PMDETA addition. Ethyl bromodifluoroacetate (2.5 mL, 19.8 mmol, 1.5 eq) and a solution of **11** (3.8 g, 13 mmol, 1 eq) in acetonitrile (5 mL) were then added dropwise via dropping funnel and the mixture was heated at 100 °C for 12 hours. The reaction was filtered over celite washing with EtOAc and concentrated under reduced pressure. Purification by flash chromatography (9:1 hexane/EtOAc) afforded the title ester (5.4 g, 79%) as colourless oil as a 5:1 mixture of *E*/*Z* isomers. (*Z* isomer resonances are denoted by an asterisk). R_f 0.44 (9:1 hexane/EtOAc); ^{1}H NMR (400 MHz, $CDCl_3$): δ = 8.08 – 8.01 (m, 2.4H), 7.59 – 7.50 (m, 1.2 H), 7.48 – 7.39 (m, 2.4H), 6.33 – 6.20 (m, 1H), 6.07 – 5.78* (m, 0.2H), 5.73 – 5.61 (m, 1H), 5.60 – 5.49* (m, 0.2H), 4.36 – 4.26 (m, 4.4H), 2.32 – 2.22* (m, 0.4H), 2.19 – 2.07 (m, 2H), 1.75 (p, 2.4H), 1.52 – 1.15 (m, 20.4H); ^{13}C NMR (100 MHz, $CDCl_3$): 166.80, 164.4* (t, *J* = 35 Hz) , 164.3 (t, *J* = 34.8 Hz), 142.5* (t, *J* = 7.1 Hz), 140.1 (t, *J* = 9.0 Hz), 132.9, 130.7, 129.7, 128.4, 121.1 (t, *J* = 25.0 Hz), 121.0* (t, *J* = 26.4 Hz), 113.0* (t, *J* = 248.7 Hz), 112.52 (t, *J* = 247.5 Hz), 65.2, 63.0, 32.0, 29.6, 29.5 (2C), 29.4 (2C), 29.3*, 29.1, 28.8, 28.5*, 28.2, 26.1, 14.1; ^{19}F NMR (376 MHz, $CDCl_3$): δ = -98.8 – -98.9* (m, 0.4 F)), -102.8 – -103.0 (m, 2F)). MS (ESI, *m/z*): calcd. for $C_{23}H_{32}FO_4$ $[M-F]^+$: 391, found 391.23; calcd. for $C_{23}H_{32}F_2O_4Na$ $[M+Na]^+$: 433.23, found 433.2

(14-Ethoxy-13,13-difluoro-14-oxo-tetradecyl) benzoate (13)

10% Pd/C (100 mg) was added to a degassed solution of **12** (1 g) in THF (10 mL); the round-bottom flask was purged with hydrogen and stirred

overnight at room temperature. The reaction mixture was filtered over celite and concentrated under pressure affording the title compound (1 g, quantitative) as a colourless oil. R_f 0.43 (9:1 hexane/EtOAc); ^{1}H NMR (400 MHz, $CDCl_3$): δ = 8.10-8.00 (m, 2H), 7.58 -7.50 (m, 1H), 7.47-7.39 (m, 2H), 4.36-4.28 (m, 4H), 2.12-1.96 (m, 2H), 1.77 (p, *J* = 6.8 Hz, 2H), 1.50-1.39 (m, 4H), 1.39-1.18 (m, 17H); ^{13}C NMR (100 MHz, $CDCl_3$): δ = 166.8, 164.6 (t, *J* = 33.3 Hz), 132.9, 130.7, 129.7, 128.5, 116.6 (t, *J* = 249.9 Hz), 65.3, 62.8, 34.6 (t, *J* = 23.3 Hz), 29.8, 29.7 (2C), 29.5, 29.4 (2C), 29.2, 28.9, 26.2, 21.6 (t, *J* = 4.1 Hz), 14.1; ^{19}F NMR (376 MHz, $CDCl_3$): δ = -105.90 (t, *J* = 16.9 Hz); MS (ESI, *m/z*): calcd. for $C_{23}H_{34}F_2O_4Na$ $[M+Na]^+$: 435.24, found 435.2.

(13,13-Difluoro-14-hydroxy-tetradecyl) benzoate (14)

Sodium borohydride (86 mg, 2.25 mmol, 1 eq) was added portion wise to a solution of **13** (930 mg, 2.25 mmol, 1 eq) in ethanol (10 mL) cooled to 0 °C. After 1 hour of stirring at room temperature the reaction was quenched with sat. aq. NH_4Cl solution and the mixture was extracted with EtOAc; the organic layer was washed with brine, dried over Na_2SO_4 and concentrated under reduced pressure. Purification by flash chromatography (8:2 hexane/EtOAc) afforded the title compound (765 mg, 94%) as white solid. R_f 0.35 (8:2 hexane/EtOAc); ^{1}H NMR (400 MHz, $CDCl_3$): δ = 8.08-8.00 (m, 2H), 7.60 -7.51 (m, 1H), 7.48-7.39 (m, 2H), 4.31 (t, *J* = 6.7 Hz, 2H), 3.73 (td, *J* = 12.8 Hz, 6.7 Hz, 2H), 1.98-1.82 (m, 2H), 1.81-1.71 (p, *J* = 6.6 Hz, 2H), 1.59 (br s, 1H), 1.54-1.40 (m, 4H), 1.40-1.19 (m, 14H); ^{13}C NMR (100 MHz, $CDCl_3$): δ = 166.9, 132.9, 130.7, 129.7, 128.5, 123.5 (t, *J* = 239.8 Hz), 65.3, 64.2 (t, *J* = 31.8 Hz), 33.4 (t, *J* = 23.8 Hz), 29.7, 29.5 (2C), 29.5 (3C), 29.4, 28.9, 26.2, 21.9 (t, *J* = 4.4 Hz); ^{19}F NMR (376 MHz, $CDCl_3$): δ = -108.60 (tt, *J* = 17.3 Hz, 12.7 Hz); MS (ESI, *m/z*): calcd. for $C_{21}H_{32}F_2O_3Na$ $[M+Na]^+$: 393.23, found 393.2; calcd. for $C_{21}H_{33}F_2O_3$ $[M+H]^+$: 371.23, found 371.2.

16-Ethoxy-13,13-difluoro-14-hydroxy-16-oxohexadecyl benzoate (15)

Compound synthesised according to a modified reported procedure.[58,59] DMSO (2.4 mL, 33.4 mmol, 6 eq) in DCM (24 mL) was cooled to -78 °C, oxalyl chloride (1.5 mL, 16.7 mmol, 3 eq) was carefully added dropwise and the solution was vigorously stirred for 2 minutes at the same temperature. A solution of **14** (2.06 g, 5.56 mmol, 1 eq) in DCM (10 mL) was then added via dropping funnel over 10 minutes. The resulting mixture was vigorously stirred for one hour at -78 °C, before TEA (6.4 mL, 45.96 mmol, 12 eq) was added via dropping funnel over 10 minutes. The reaction mixture was stirred for additional 30 minutes at -78 °C and allowed to warm to room temperature in one hour via removal of the external cooling bath. The reaction was quenched with sat. aq. NH_4Cl solution, diluted with water and extracted with DCM. The combined organic layers were washed with sat. aq. $NaHCO_3$ solution, water, brine, dried over Na_2SO_4 and concentrated under reduced pressure to give the crude aldehyde as a yellow oil. The crude product was used without further purification. Zinc dust (871 mg, 13.3 mmol, 2.5 eq) was suspended in THF (27 mL) and the suspension stirred for 5 minutes. TMSCl (250 µL, 2 mmol, 0.375 eq) was then added and the resulting mixture stirred for 15 minutes. The reaction was gently heated with the heat gun for 1 minute under nitrogen flow and allowed to cool back to room temperature (three times). A solution of the freshly prepared aldehyde (2.06 g, 5.3 mmol, 1 eq) in THF (10 mL) and ethyl bromoacetate (880 µL, 8.0 mmol, 1.5 eq) were consecutively dropwise added and the resulting suspension was refluxed for 1.5 hours. The reaction was quenched with sat. aq. NH_4Cl solution, filtered over celite and extracted with Et_2O. The combined organic layers were washed with water, brine, dried over Na_2SO_4 and concentrated under reduced pressure. Purification by flash chromatography (8:2 hexane/EtOAc) afforded the title β-hydroxy-ester (750 mg, 30% over two steps) as a yellow oil. R_f 0.35 (8:2 hexane/EtOAc); ^{1}H NMR (400 MHz, $CDCl_3$): δ = 8.04 (dd, *J* = 8.4, 1.4 Hz, 2H), 7.55 (t, *J* = 7.4 Hz, 1H), 7.43 (t, *J* = 7.6 Hz, 2H), 4.31 (t, *J* = 6.6 Hz, 2H), 4.24 – 4.08 (m, 3H), 3.34 (d, *J* = 5.3 Hz, 1H), 2.70 (dd, *J* = 16.6, 3.1 Hz, 1H), 2.60 (dd, *J* = 16.7, 9.2 Hz, 1H), 2.03 – 1.85 (m, 2H), 1.82 – 1.70 (m, 2H), 1.57 – 1.38 (m, 4H), 1.39 – 1.21 (m, 17H); ^{13}C NMR (100 MHz, $CDCl_3$): δ = 172.5, 166.8, 132.9, 130.7, 129.7, 128.4, 123.6 (dd, *J* = 246.9, 242.5 Hz), 69.4 (dd, *J* = 33.3, 27.3 Hz), 65.3, 61.3, 34.6 (t, *J* = 3.3 Hz), 32.9 (t, *J* = 23.9 Hz), 29.7, 29.6 (3C), 29.5 (2C), 29.4, 28.8, 26.2, 21.5 (dd, *J* = 6.0, 3.2 Hz), 14.2; ^{19}F NMR (376 MHz, $CDCl_3$): δ = -109.0 – -110.3 (m, 1F), -113.4 – -114.6 (m, 1F); MS (ESI, *m/z*): calcd. for $C_{25}H_{38}F_2O_5Na$ $[M+Na]^+$: 479.27, found 479.3; calcd. for $C_{25}H_{39}F_2O_5$ $[M+H]^+$: 457.27, found 457.3.

[(*E*)-16-Ethoxy-13,13-difluoro-16-oxo-hexadec-14-enyl] benzoate (15a)

TEA (93 µL, 0.67 mmol, 2.5 eq) and MsCl (31 µL, 0.40 mmol, 1.5 eq) were added dropwise to a solution of **15** (122 mg, 0.27 mmol, 1 eq) in DCM (1.2 mL) cooled to 0 °C. The reaction was stirred for 12 hours at room temperature. The mixture was then cooled 0 °C, DBU (80 µL, 0.53 mmol, 2 eq) was added dropwise and the mixture was stirred for 2 additional hours at room temperature. The reaction was quenched with sat. aq. $NaHCO_3$ solution and extracted with DCM. The organic layer was washed with sat. aq. $NaHCO_3$ solution and brine, dried over Na_2SO_4 and concentrated under reduced pressure. Purification by flash chromatography (95:5 hexane/EtOAc) afforded the title α,β-unsaturated ester (92 mg, 78%) as a colourless oil. R_f 0.27 (95:5 hexane/EtOAc); ^{1}H NMR (400 MHz, $CDCl_3$): δ = 8.1 – 8.0 (m, 2H), 7.6 – 7.5 (m, 1H), 7.4 (dd, *J* = 8.3, 7.0 Hz, 2H), 6.8 (dt, *J* = 15.8, 11.3 Hz, 1H), 6.2 (dt, *J* = 15.8, 2.2 Hz, 1H), 4.3 (t, *J* = 6.7 Hz, 2H), 4.2 (q, *J* = 7.1 Hz, 2H), 2.0 – 1.8 (m, 2H), 1.8 – 1.7 (m, 2H), 1.5 – 1.4 (m, 4H), 1.4 – 1.2 (m, 17H); ^{13}C NMR (100 MHz, $CDCl_3$): δ = 166.8, 165.3, 139.7 (t, *J* = 27.8 Hz), 132.9, 130.6, 129.6, 128.4, 124.9 (t, *J* = 8.4 Hz), 120.8 (t, *J* = 239.6 Hz), 65.2, 61.2, 37.2 (t, *J* = 25.6 Hz), 29.6 (3C), 29.5, 29.4 (2C), 29.3, 28.8, 26.1, 22.2 (t, *J* = 4.1 Hz), 14.3; ^{19}F NMR (376 MHz, $CDCl_3$): δ = -98.3 – -98.8 (m, 2F); MS (ESI, *m/z*): calcd. for $C_{25}H_{36}F_2O_4Na$ $[M+Na]^+$: 461.26, found 461.2; calcd. for $C_{25}H_{37}F_2O_4$ $[M+H]^+$: 439.26, found 439.3.

(16-Ethoxy-13,13-difluoro-16-oxo-hexadecyl) benzoate (16)

10% Pd/C (6 mg) was added to a degassed solution of **15a** (57 mg) in THF (1 mL); the reaction mixture was purged with hydrogen and stirred for 2 hours at room temperature. The reaction mixture was filtered over celite and concentrated under pressure affording the title compound (57 mg, quantitative) as a colourless oil. R_f 0.39 (9:1 hexane/EtOAc); ^{1}H NMR (400 MHz, $CDCl_3$): δ = 8.07-7.99 (m, 2H), 7.58 -7.50 (m, 1H), 7.47-7.38 (m, 2H), 4.31 (t, *J* = 6.7 Hz, 2H), 4.14 (q, *J* = 7.1 Hz, 2H), 2.50 (t, *J* = 7.6 Hz, 2H), 2.25-2.08 (m, 2H), 1.89-1.70 (m, 4H), 1.51-1.39 (m, 4H), 1.39-1.1 (m, 17H); ^{13}C NMR (100 MHz, $CDCl_3$): δ = 172.6, 166.8, 132.9, 130.7, 129.6, 128.4, 124.5 (t, *J* = 239.1 Hz), 65.2, 60.8, 36.8 (t, *J* = 24.8 Hz), 31.7 (t, *J* = 25.8 Hz), 29.7, 29.6 (3C), 29.5, 29.4 (2C), 28.8, 27.4 (t, *J* = 4.8 Hz), 26.2, 22.4 (t, *J* = 4.5 Hz), 14.3; ^{19}F NMR (376 MHz, $CDCl_3$): δ = -99.78 (p, *J* = 16.7 Hz); MS (ESI, *m/z*): calcd. for $C_{25}H_{38}F_2O_4Na$ $[M+Na]^+$: 463.27, found 463.2; calcd. for $C_{25}H_{39}F_2O_4$ $[M+H]^+$: 441.27, found 441.3.

Ethyl 4,4-difluoro-16-hydroxy-hexadecanoate (17)

Sodium Ethoxide 21% in ethanol (44 µL, 0.12 mmol, 1.2 eq) was added dropwise to a solution of **16** (43 mg, 98 µmol, 1 eq) in ethanol (1 mL) cooled to 0 °C. After stirring for five hours at room temperature the reaction was quenched with sat. aq. NH_4Cl solution and the mixture was extracted with EtOAc. The organic layer was washed with brine, dried over Na_2SO_4 and concentrated under reduced pressure. Purification by flash chromatography (7:3 hexane/EtOAc) afforded the title compound (30 mg, 91%) as a white solid. (OH signal was not observed). R_f 0.36 (7:3 hexane/EtOAc); ^{1}H NMR (400 MHz, $CDCl_3$): δ = 4.14 (q, *J* = 7.2 Hz, 2H), 3.62 (t, *J* = 6.7 Hz, 2H), 2.50 (t, *J* = 7.5 Hz, 2H), 2.25-2.07 (m, 2H), 1.90-1.72 (m, 2H), 1.63-1.51 (m, 2H), 1.51-1.40 (m, 4H), 1.38-1.16 (m, 17H); ^{13}C NMR (100 MHz, $CDCl_3$): δ = 172.7, 124.5 (t, *J* = 239.2 Hz), 63.2, 60.8, 36.8 (t, *J* = 24.8 Hz), 32.9, 31.7 (t, *J* = 25.8 Hz), 29.7 (2C), 29.6, 29.5 (3C), 29.4, 27.4 (t, *J* = 4.8 Hz), 25.9, 22.4 (t, *J* = 4.5 Hz), 14.3; ^{19}F NMR (376 MHz, $CDCl_3$): δ = -99.79 (p, *J* = 16.7 Hz); MS (ESI, *m/z*):

calcd. for $C_{18}H_{34}F_2O_3Na$ $[M+Na]^+$: 359.25, found 359.2; calcd. for $C_{18}H_{35}F_2O_3$ $[M+H]^+$: 337.25, found 337.3.

Ethyl 4,4-difluoro-16-(tosyloxy)hexadecanoate (18)

To a solution of **17** (438 mg, 1.30 mmol, 1 eq), DMAP (23 mg, 0.20 mmol, 0.1 eq) and TEA (270 µL, 1.95 mmol, 1.5 eq) in DCM (3 mL) cooled to 0 °C was dropwise added a solution of tosyl chloride (372 mg, 1.95 mmol, 1.5 eq) in DCM (2 mL) and the reaction was stirred for 4 hours at room temperature. The reaction was quenched with sat. aq. $NaHCO_3$ solution and extracted with DCM. The organic layer was washed with sat. aq. $NaHCO_3$ solution, brine, dried over Na_2SO_4 and concentrated under reduced pressure. Purification by flash chromatography (85:15 hexane/EtOAc) afforded the title compound (610 mg, 96%) as a white solid. R_f 0.4 (8:2 hexane/EtOAc); ^{1}H NMR (400 MHz, $CDCl_3$): δ = 7.77 (d, J = 8.3 Hz, 2H), 7.33 (d, J = 8.0 Hz, 2H), 4.13 (q, J = 7.1 Hz, 2H), 4.00 (t, J = 6.5 Hz, 2H), 2.49 (d, J = 8.0 Hz, 2H), 2.43 (s, 3H), 2.24 – 2.07 (m, 2H), 1.80 (q, J = 16.4 Hz, 2H), 1.61 (p, J = 6.6 Hz, 2H), 1.51 – 1.38 (m, 2H), 1.33 – 1.17 (m, 19H); ^{13}C NMR (100 MHz, $CDCl_3$): δ = 172.6, 144.7, 133.4, 129.9, 128.0, 124.5 (t, J = 240.8 Hz), 70.8, 60.8, 36.8 (t, J = 25.0 Hz), 31.6 (t, J = 25.9 Hz), 29.6, 29.5 (2C), 29.4 (3C), 29.0, 28.9, 27.4 (t, J = 4.8 Hz), 25.4, 22.4, 22.3, 21.7, 14.3; ^{19}F NMR (376 MHz, $CDCl_3$): δ = -99.8 (p, J = 16.8 Hz); MS (ESI, *m/z*): calcd. for $C_{25}H_{40}F_2O_5SNa$ $[M+Na]^+$: 513.26, found 513.2; calcd. for $C_{25}H_{40}FO_5S$ $[M-F]^+$: 471.26, found 471.2.

Radiochemistry

Labelling with tritium

Tritium gas was obtained from RC Tritec (2.12 GBq/µmol, 1.06 GBq/µatom) and was handled on a RC Tritec tritium manifold. Analytical high-performance liquid chromatography (HPLC) was performed using a Waters Acquity HPLC system with in-line detection of radioactivity using a lab Logic BetaRam model 5. Liquid scintillation counting was performed with a Beckman LS 6500 scintillation counter.

[^{3}H]Ethyl 4,4,16-trifluorohexadecanoate ([^{3}H]9a)

Compound **10** (3 mg, 8.92 µmol) and 10% Pd/C (2 mg) were combined in THF (0.5 mL). The mixture was frozen using liquid nitrogen and the flask evacuated before closing the vacuum tap and being allowed to warm to RT. This was performed twice. The mixture was frozen once more and the flask evacuated, then tritium gas was released from the uranium bed by heating it with a blow torch. The mixture was allowed to warm to RT and stirred for 2 hours under tritium gas atmosphere (276.6 GBq). The solvent was removed under a nitrogen stream, the residue was diluted with 0.5 mL of ethanol and evaporated (repeated twice) to remove the labile tritium. The residue was diluted with ethanol, filtered (0.45 µm PTFE filter) and reconstituted in ethanol (30 mL) to give the crude product (30.9 GBq, radiochemical purity 83%). A portion of the crude (4 GBq) were purified by reversed phase preparative HPLC: column XBridge BEH C18 OBD Prep Column, 130Å, 5 µm, 19 mm X 100 mm; solvents A water +0.1% TFA, B acetonitrile; gradient 70% B to 85% B in 10 minutes; flow 10 mL/min. The purified fractions were dried under vacuum and reconstituted in 10 mL of ethanol to give the purified ester (1.5 GBq, radiochemical purity 98.6%) as a solution that was stored at -20 °C.

[^{3}H]4,4,16-Trifluorohexadecanoic acid ([^{3}H]1)

To a solution of purified [^{3}H]**9a** (725 MBq) in THF (100 µL) and water (100 µL) were added 100 microliters of a 10 mg/mL solution of lithium hydroxide in water (1 mg) and the reaction was stirred overnight at room temperature. Reaction was monitored by HPLC and finished after 12 h. The mixture was acidified with 100 microliters of HCl 1N, diluted with ACN and the solvent removed by rotary evaporation. The crude acid (495.7 MBq) was reconstituted in 10 mL of acetonitrile and purified by reversed phase preparative HPLC: column XBridge BEH C18 OBD Prep Column, 130Å, 5 µm, 19 mm X 250 mm; solvents A water +0.1% TFA, B acetonitrile; gradient 50% B to 100% B in 15 minutes; flow 10 mL/min. The purified fractions were dried under vacuum and reconstituted in 10 mL of acetonitrile to give the purified acid (367 MBq, radiochemical purity > 99%.) as a solution that was stored at -20 °C. ^{3}H NMR (533 MHz, CD_3OD): δ = 1.84 (m, 0.05 T) 1.45 (m, 0.3 T), 1.25 (m, 1 T).

Molar activity calculation

The molar activity of the tritiated tracer was determined according to the protocol reported by Schenk et al.[48] Tritiated canagliflozin (molar activity 1.3 GBq/mmol), synthesised by AstraZeneca, was used as internal standard in the NMR experiments. Its radiochemical purity was 91.71%, as determined by radio-HPLC. An NMR tube containing 100 MBq of tritiated canagliflozin and 100 MBq of [^{3}H]**1** dissolved in deuterated methanol was prepared and ^{1}H/^{3}H NMR spectra were acquired. ^{3}H NMR-based radioactive concentration of the analyte was calculated from the sum of the proton-decoupled tritium NMR integral for canagliflozin (7.18 ppm 1.00 T, 6.76 ppm 0.98 T, sum 1.98 T) and [^{3}H]**1** (1.46 – 1.21 ppm, 2.99 T). The analyte moles in the sample were determined using the aromatic canagliflozin proton integral (7.56 ppm, 2H) as standard, along with the analyte resonance of the methylene group bearing a primary fluoride (4.42 ppm, 1.47 H). The calculated [^{3}H]**1** radioactivity concentration was 44 MBq/mL and 0.05 µmol of analyte were found in the sample. The calculated molar radioactivity was 2730 GBq/mmol.

Labelling with fluorine

[^{18}F]4,4,16-Trifluorohexadecanoic acid ([^{18}F]1)

The fluorine labelling was performed with a TRACERlab FX_{FN} synthesiser (GE Healthcare). [^{18}F]Fluoride was produced by proton irradiation of ^{18}O-enriched water with 18MeV protons using a Cyclone 18/9 cyclotron (IBA). After the end of bombardment (EOB), [^{18}F]Fluoride was transferred into a ventilated and lead-shielded hot cell where it was trapped on a preconditioned Sep-Pak© Accell Plus QMA Plus Light cartridge (Waters, Milford, MA, USA) and eluted in the reaction vessel with 500 µL of a 7 mg/mL potassium carbonate solution in water; a solution of Kryptofix© 222 (15 mg) in acetonitrile (1 mL) was then added in the vessel. After azeotropic drying of the solvent, a solution of compound **18** (5 mg) in acetonitrile (300 µL) was added and the mixture was heated at 90 °C for 15 minutes. Afterwards, the vessel was cooled at room temperature before addition of KOH 0.2 N aqueous solution (180 µL) and subsequent heating at 90 °C for 15 minutes. The reaction was then cooled at room temperature and the crude mixture was acidified with HCl 1 M aqueous solution (60 µL), diluted with a mixture of acetonitrile and water (7/3, 2 mL) and purified by reversed phase semipreparative HPLC: column Teknokroma Mediterranea Sea18, 5 µm, 250 mm x 10 mm; solvents A water, B acetonitrile + 0.1% TFA; gradient 70% B isocratic; flow rate 5 mL/min. The desired fraction (Rt = 15.8 min.) was collected, diluted with water (20 mL) and the radiotracer was trapped on a C18 cartridge (Sep-Pak© Light, Waters, Milford, MA, USA). The cartridge was washed with water (5 mL) before elution with ethanol (1 mL) yielding the final radiotracer solution, which was diluted with 1% BSA in physiological saline solution (1:9, v:v) before injection into animals. Radiochemical purity and tracer identity were determined by HPLC, using an Agilent 1200 Series system equipped with a variable wavelength UV detector and a radioactivity detector (Gabi, Raytest). A Phenomenex Luna® C18 column (5 µm, C18, 100 Å, 250 x 4.6 mm) was used as the stationary phase and water (A)/acetonitrile containing 0.1% TFA (B) were used as the mobile phase, using the following gradient: 0 min 80% B; 20 min 100% B; 23 min 100% B. The flow was set to 1 mL/min. Overall production time was typically 1 hour and 10 minutes from EOB and the radiochemical yields were in the range 10-15% decay corrected. Radiochemical purity was higher than 99%. Identity of the product was confirmed by comparison with non-radioactive reference **1** (Figure S1a).

In vitro metabolism

Metabolism of [^{3}H]**1** was measured by incubating rat liver microsomes (0.1mg of protein; Thermo-Fisher Scientific) in a reaction mixture containing the labelled fatty acid (0.36 MBq; 13 nmol) in 0.12M potassium phosphate buffer pH 7.4. The enzymatic reaction was initiated by the addition of 10 µl freshly prepared 20 mM NADPH in 0.12M potassium phosphate buffer, pH 7.4. At pre-selected time points (15, 30, 60, and120 min), the reaction was terminated by the addition of 100 µl of acetonitrile. Samples were centrifuged at 5800 rpm for 5 min to pellet the precipitated protein. The resulting supernatants were analyzed by HPLC, using an Agilent 1200 Series chromatograph equipped with a multiple wavelength UV detector (λ = 254 nm) and radioactivity detector (Ramona, Raytest) equipped with an internal solid scintillation cell. HPLC conditions were the same as above for quality control.

Animal experiments

Drug challenge with etomoxir

Animals were maintained and handled in accordance with the Guidelines for Accommodation and Care of Animals (European Convention for the Protection of Vertebrate Animals Used for Experimental and Other Scientific Purposes). All animal procedures were performed in accordance with the European Union Animal Directive (2010/63/EU). Experimental procedures were approved by (i) the internal ethical committee at CIC biomaGUNE; (ii) an accredited, external ethical committee (Órgano Habilitado del IIS Biodonostia); and (iii) local authorities (Diputación Foral de Guipuzcoa) (project code: PRO-AE-SS-059).

Blood clearance and *in vivo* metabolism were determined in rats (Sprague Dawley rats; weight between 188 g and 231 g; n=2). For imaging studies, animals (Sprague Dawley rats; weight between 188 g and 231 g; n=10) were fasted for 12 hours before imaging studies. After fasting, animals were divided in two groups called “Etomoxir” and “Control” (n=5 per group). In “etomoxir” group, rats received an intraperitoneal (I.P.) injection of etomoxir (Fluorochem; 40 mg/kg, solution in physiological saline solution containing 5% of DMSO; stored at 37°C) 2 hours before administration of [^{18}F]**1**. Animals included in the “Control” group received an I.P. injection of an equivalent volume of vehicle at the same time point.

PET imaging studies

Animals were anesthetized by inhalation of isoflurane in pure oxygen (5% for induction; 1-2% for maintenance). The animal was positioned with the heart centred in the middle of the field of view of the PET scanner (β-CUBE Molecubes preclinical platform), and the radiotracer (5.5-7.5 MBq; 250-300 µL) was administered through the tail vein concomitantly with the start of image acquisition (60 min, list mode; effective field of view: 10.5 cm). After finalising the PET imaging session, a whole-body CT scan (β-CUBE Molecubes preclinical platform) was acquired. PET data were reconstructed by 3D-OSEM iterative image reconstruction algorithm (30 iterations, with a reconstructed voxel size of 400 µm) and processed with PMOD (PMOD Technologies LLC) software analysis tool. The same software was used to co-register the PET and the CT images. Volumes of interest (VOIs) were drawn in the myocardium, liver, kidneys, lungs and cava vein. Dynamic TACs were obtained over the whole duration of the scan.

Acknowledgements

We thank the European Union’s Horizon 2020 research and innovation programme under the Marie Sklodowska-Curie grant agreement N° 675417 (PET3D project) for financial support of the project and the studentship of A.C. and R.P. J.L. acknowledges the Spanish Ministry of Economy and Competitiveness (CTQ2017-87637-R). Part of the work was conducted under the Maria de Maeztu Units of Excellence Programme – Grant No. MDM-2017-0720. We are grateful to Annika Langborg Weinmann for assistance with the purification of **1**.

Conflict of interest

The authors declare no conflict of interest.

Keywords: PET Imaging • Fatty acids • Radiopharmaceuticals • Heart Failure • Palmitate

[1] C. W. Yancy, M. Jessup, B. Bozkurt, J. Butler, D. E. Casey, M. H. Drazner, G. C. Fonarow, S. A. Geraci, T. Horwich, J. L. Januzzi, M. R. Johnson, E. K. Kasper, W. C. Levy, F. A. Masoudi, P. E. McBride, J. J. V. McMurray, J. E. Mitchell, P. N. Peterson, B. Riegel, F. Sam, L. W. Stevenson, W. H. W. Tang, E. J. Tsai, B. L. Wilkoff, *J. Am. Coll. Cardiol.* **2013**, *62*, 1495–1539.
[2] G. Savarese, L. H. Lund, *Card. Fail. Rev.* **2017**, *3*, 7–11.
[3] W. C. Stanley, F. A. Recchia, G. D. Lopaschuk, *Physiol. Rev.* **2005**, *85*, 1093–1129.
[4] T. Doenst, T. D. Nguyen, E. D. Abel, *Circ. Res.* **2013**, *113*, 709–724.
[5] J. C. Shipp, L. H. Opie, D. Challoner, *Nature* **1961**, *189*, 1018–1019.
[6] G. D. Lopaschuk, D. D. Belke, J. Gamble, I. Toshiyuki, B. O. Schönekess, *Biochim. Biophys. Acta BBA - Lipids Lipid Metab.* **1994**, *1213*, 263–276.
[7] J. R. Neely, H. E. Morgan, *Annu. Rev. Physiol.* **1974**, *36*, 413–459.
[8] G. D. Lopaschuk, J. R. Ussher, C. D. L. Folmes, J. S. Jaswal, W. C. Stanley, *Physiol. Rev.* **2010**, *90*, 207–258.
[9] T. R. DeGrado, F. Bhattacharyya, M. K. Pandey, A. P. Belanger, S. Wang, *J. Nucl. Med.* **2010**, *51*, 1310–1317.
[10] T. R. DeGrado, H. H. Coenen, G. Stöcklin, *J. Nucl. Med.* **1991**, *32*, 1888–1896.
[11] Z. Cai, N. S. Mason, C. J. Anderson, W. B. Edwards, *Nucl. Med. Biol.* **2016**, *43*, 108–115.
[12] M. K. Pandey, A. P. Belanger, S. Wang, T. R. DeGrado, *J. Med. Chem.* **2012**, *55*, 10674–10684.
[13] Aubert Gregory, Martin Ola J., Horton Julie L., Lai Ling, Vega Rick B., Leone Teresa C., Koves Timothy, Gardell Stephen J., Krüger Marcus, Hoppel Charles L., Lewandowski E. Douglas, Crawford Peter A., Muoio Deborah M., Kelly Daniel P., *Circulation* **2016**, *133*, 698–705.
[14] Sack Michael N., Rader Toni A., Park Sonhee, Bastin Jean, McCune Sylvia A., Kelly Daniel P., *Circulation* **1996**, *94*, 2837–2842.
[15] L. Chen, J. Song, S. Hu, *Heart Fail. Rev.* **2019**, *24*, 143–154.
[16] Kolwicz Stephen C., Purohit Suneet, Tian Rong, *Circ. Res.* **2013**, *113*, 603–616.
[17] E. Bertero, C. Maack, *Nat. Rev. Cardiol.* **2018**, *15*, 457–470.
[18] S. M. Ametamey, M. Honer, P. A. Schubiger, *Chem. Rev.* **2008**, *108*, 1501–1516.
[19] D. J. Hnatowich, *J. Cell. Biochem.* **2002**, *87*, 18–24.
[20] *Radiopharmaceutical Chemistry*, Springer Berlin Heidelberg, New York, NY, **2018**.
[21] M. K. Pandey, A. Bansal, T. R. DeGrado, *Heart Metab* **2011**, *51*, 15–19.
[22] K. J. Mather, T. R. DeGrado, *Biochim. Biophys. Acta BBA - Mol. Cell Biol. Lipids* **2016**, *1861*, 1535–1543.
[23] E. S. Weiss, E. J. Hoffman, M. E. Phelps, M. J. Welch, P. D. Henry, M. M. Ter-Pogossian, B. E. Sobel, *Circ. Res.* **1976**, *39*, 24–32.

[24] R. A. Lerch, H. D. Ambos, S. R. Bergmann, M. J. Welch, M. M. Ter-Pogossian, B. E. Sobel, *Circulation* **1981**, *64*, 689–699.
[25] H. R. Schelbert, E. Henze, R. Keen, H. R. Schon, H. Hansen, C. Selin, S.-C. Huang, J. R. Barrio, M. E. Phelps, *Am. Heart J.* **1983**, *106*, 736–750.
[26] N. L. Christensen, S. Jakobsen, A. C. Schacht, O. L. Munk, A. K. O. Alstrup, L. P. Tolbod, H. J. Harms, S. Nielsen, L. C. Gormsen, *Mol. Imaging* **2017**, *16*, 1536012117734485.
[27] R. J. Gropler, *Circ. Cardiovasc. Imaging* **2010**, *3*, 211–222.
[28] S. R. Bergmann, C. J. Weinheimer, J. Markham, P. Herrero, *J. Nucl. Med.* **1996**, *37*, 1723–1730.
[29] T. L. Rosamond, D. R. Abendschein, B. E. Sobel, S. R. Bergmann, K. A. Fox, *J. Nucl. Med. Off. Publ. Soc. Nucl. Med.* **1987**, *28*, 1322–1329.
[30] E. J. Knust, C. Kupfernagel, G. Stöcklin, *J. Nucl. Med.* **1979**, *20*, 1170–1175.
[31] E. Livni, D. R. Elmaleh, S. Levy, G. L. Brownell, W. H. Strauss, *J. Nucl. Med.* **1982**, *23*, 169–175.
[32] T. Takahashi, S.-I. Nishimura, T. Ido, K.-I. Ishiwata, R. Iwata, *Nucl. Med. Biol.* **1996**, *23*, 303–308.
[33] B. Renstrom, S. Rommelfanger, C. K. Stone, T. R. DeGrado, K. J. Carlson, E. Scarbrough, R. J. Nickles, A. J. Liedtke, J. E. Holden, *J. Nucl. Med.* **1998**, *39*, 1684–1689.
[34] T. R. DeGrado, S. Wang, J. E. Holden, R. J. Nickles, M. Taylor, C. K. Stone, *Nucl. Med. Biol.* **2000**, *27*, 221–231.
[35] S. S. Pochapsky, H. F. VanBrocklin, M. J. Welch, J. A. Katzenellenbogen, *Bioconjug. Chem.* **1990**, *1*, 231–244.
[36] T. M. Shoup, D. R. Elmaleh, A. A. Bonab, A. J. Fischman, *J. Nucl. Med.* **2005**, *46*, 297–304.
[37] L. A. Reiter, G. J. Martinelli, L. A. Reeves, P. G. Mitchell, *Bioorg. Med. Chem. Lett.* **2000**, *10*, 1581–1584.
[38] G. A. Patani, E. J. LaVoie, *Chem. Rev.* **1996**, *96*, 3147–3176.
[39] J. Atzrodt, V. Derdau, W. J. Kerr, M. Reid, *Angew. Chem. Int. Ed.* **2018**, *57*, 1758–1784.
[40] C. S. Elmore, **2009**, *44*, 515–534.
[41] S. Karabiyikoglu, R. G. Iafe, C. A. Merlic, *Org. Lett.* **2015**, *17*, 5248–5251.
[42] X. Wang, S. Zhao, J. Liu, D. Zhu, M. Guo, X. Tang, G. Wang, *Org. Lett.* **2017**, *19*, 4187–4190.
[43] D. H. R. Barton, S. W. McCombie, *J. Chem. Soc. Perkin 1* **1975**, *0*, 1574–1585.
[44] D. H. R. Barton, O. J. Doo, J. Cs. Jaszberenyi, *Tetrahedron Lett.* **1990**, *31*, 4681–4684.
[45] M. Yasuda, Y. Onishi, M. Ueba, T. Miyai, A. Baba, *J. Org. Chem.* **2001**, *66*, 7741–7744.
[46] W. S. Mahoney, D. M. Brestensky, J. M. Stryker, *J. Am. Chem. Soc.* **1988**, *110*, 291–293.
[47] P. W. Miller, N. J. Long, R. Vilar, A. D. Gee, *Angew. Chem. Int. Ed.* **2008**, *47*, 8998–9033.
[48] D. J. Schenk, P. G. Dormer, D. Hesk, S. R. Pollack, C. F. Lavey, *J. Label. Compd. Radiopharm.* **2015**, *58*, 291–298.
[49] C. S. Elmore, D. J. Schenk, R. Arent, L. Kingston, *J. Label. Compd. Radiopharm.* **2014**, *57*, 645–651.
[50] Y. Amet, F. Adas, F. Berthou, *Anal. Chim. Acta* **2002**, *465*, 193–198.
[51] L. Hammerer, C. K. Winkler, W. Kroutil, *Catal. Lett.* **2018**, *148*, 787–812.
[52] C.-H. Chiang, R. Ramu, Y.-J. Tu, C.-L. Yang, K. Y. Ng, W.-I. Luo, C. H. Chen, Y.-Y. Lu, C.-L. Liu, S. S.-F. Yu, *Chem. – Eur. J.* **2013**, *19*, 13680–13691.
[53] K. Serdons, A. Verbruggen, G. M. Bormans, *Methods* **2009**, *48*, 104–111.
[54] F. Guarra, A. Terenzi, C. Pirker, R. Passannante, D. Baier, E. Zangrando, V. Gómez, T. Biver, C. Gabbiani, W. Berger, J. Llop, L. Salassa, *Angew. Chem. Int. Ed.* **n.d.**, *n/a*, DOI 10.1002/anie.202008046.
[55] M. S. Roberts, B. M. Magnusson, F. J. Burczynski, M. Weiss, *Clin. Pharmacokinet.* **2002**, *41*, 751–790.
[56] C. S. Patlak, R. G. Blasberg, J. D. Fenstermacher, *J. Cereb. Blood Flow Metab.* **2016**, DOI 10.1038/jcbfm.1983.1.
[57] J. Logan, J. S. Fowler, N. D. Volkow, A. P. Wolf, S. L. Dewey, D. J. Schlyer, R. R. MacGregor, R. Hitzemann, B. Bendriem, S. J. Gatley, D. R. Christman, *J. Cereb. Blood Flow Metab.* **1990**, *10*, 740–747.
[58] C. Quero, G. Rosell, O. Jiménez, S. Rodriguez, M. P. Bosch, A. Guerrero, *Bioorg. Med. Chem.* **2003**, *11*, 1047–1055.
[59] F. G. Glansdorp, G. L. Thomas, J. K. Lee, J. M. Dutton, G. P. C. Salmond, M. Welch, D. R. Spring, *Org. Biomol. Chem.* **2004**, *2*, 3329.

Entry for the Table of Contents

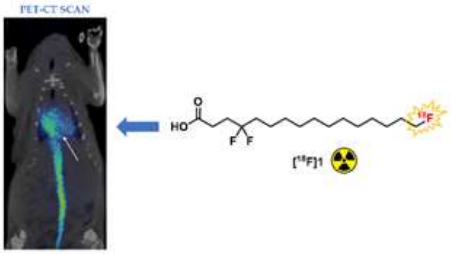

4,4,16-Trifluoropalmitate **1** was designed and synthesised as a novel metabolically trapped fatty acid oxidation PET imaging tracer for heart failure. The probe was radiolabelled with tritium and fluorine-18 and was evaluated *in vitro* as well as *in vivo*. **[^{18}F]1** showed fast clearance from the bloodstream and excellent metabolic stability, however it was not irreversibly trapped in the heart.

Researcher Twitter username: @zanda_eu